# Experimental and Model Estimates of the Contributions from Biogenic Monoterpenes and Sesquiterpenes to Secondary Organic Aerosol in the Southeastern United States

Lu Xu[1,a], Havala O.T. Pye[2], Jia He[3], Yunle Chen[3], Benjamin N. Murphy[2], Nga Lee Ng[1,3*]

[1]School of Chemical and Biomolecular Engineering, Georgia Institute of Technology, Atlanta, GA 30332, USA

[2]National Exposure Research Laboratory, US Environmental Protection Agency, Research Triangle Park, NC 27711, USA

[3]School of Earth and Atmospheric Sciences, Georgia Institute of Technology, Atlanta, GA 30332, USA

[*]To whom correspondence should be addressed. E-mail: ng@chbe.gatech.edu

[a]Present address: Division of Geological and Planetary Sciences, California Institute of Technology, Pasadena, CA 91125, USA

**Abstract**

Atmospheric organic aerosol (OA) has important impacts on climate and human health but its sources remain poorly understood. Biogenic monoterpenes and sesquiterpenes are important precursors of secondary organic aerosol (SOA), but the amounts and pathways of SOA generation from these precursors are not well constrained by observations. We propose that the less-oxidized oxygenated organic aerosol (LO-OOA) factor resolved from positive matrix factorization (PMF) analysis on aerosol mass spectrometry (AMS) data can be used as a surrogate for fresh SOA from monoterpenes and sesquiterpenes in the southeastern U.S. This hypothesis is supported by multiple lines of evidence, including lab-in-the-field perturbation experiments, extensive ambient ground-level measurements, and state-of-the-art modeling. We performed lab-in-the-field experiments, in which the ambient air is perturbed by the injection of selected monoterpenes and sesquiterpenes and subsequent SOA formation is investigated. PMF analysis on the perturbation experiments provides an objective link between LO-OOA and fresh SOA from monoterpenes and sesquiterpenes as well as insights into the sources of other OA factors. Further, we use an upgraded atmospheric model and show that modeled SOA concentrations from monoterpenes and sesquiterpenes could reproduce both the magnitude and diurnal variation of LO-OOA at multiple sites in the southeastern U.S., building confidence in our hypothesis. We estimate the annual average concentration of SOA from monoterpenes and sesquiterpenes in the southeastern U.S. to be roughly 2 $\mu g\ m^{-3}$.

## 1 Introduction

Organic aerosol (OA) constitutes a substantial fraction of ambient fine particulate matter (PM) and has large impacts on air quality, climate change, and human health (Carslaw et al., 2013; Lelieveld et al., 2015). OA can be directly emitted from sources (primary OA, POA) or formed by the oxidation of volatile organic compounds (VOCs) (secondary OA, SOA). Global measurements revealed the dominance of SOA over POA in various atmospheric environments (Jimenez et al., 2009; Ng et al., 2010). The VOCs can be emitted from natural sources (i.e., biogenic) or human activities (i.e., anthropogenic). However, the relative contribution of biogenic and anthropogenic sources to SOA formation in the atmosphere is poorly constrained. This knowledge is critical for formulating effective pollution control strategies that aim at reducing ambient PM concentrations and accurately assessing the climate effects of OA (Hallquist et al., 2009). Biogenic VOCs such as monoterpenes (MT, $C_{10}H_{16}$) and sesquiterpenes (SQT, $C_{15}H_{24}$) are recognized as critical precursors of SOA (Tsigaridis et al., 2014; Hodzic et al., 2016; Pye et al., 2010). The predicted global SOA production from MT and SQT varies from 14 to 246 Tg $yr^{-1}$ (Spracklen et al., 2011; Pye et al., 2010). This large variation in model estimates arises from a number of factors (including uncertainty in SOA yield) and introduces significant uncertainties in estimating OA concentrations and its subsequent influences on climate and human exposure.

The large model uncertainties call for ambient observations to constrain model results. Isolating and measuring SOA production from specific sources are challenging because SOA is a complex mixture consisting of thousands of compounds and SOA evolves dynamically in the atmosphere. A widely used method to apportion OA into different characteristic sources is positive matrix factorization (PMF) analysis on the organic mass spectra measured by aerosol mass spectrometer (AMS) (Ulbrich et al., 2009; Jimenez et al., 2009; Ng et al., 2010). PMF-AMS analysis groups OA constituents with similar mass spectra and temporal variations into characteristic OA subtypes (i.e., factors). This analysis has revealed that concentration of oxygenated OA (OOA), which is a surrogate of SOA, is much greater than that of hydrocarbon-like OA (HOA), which is a surrogate of POA (Zhang et al., 2007). In many circumstances especially in warmer months, more than one SOA factor is resolved from PMF analysis, often including less-oxidized oxygenated OA (LO-OOA, also denoted as semi-volatile oxygenated organic aerosol in older studies) and more-oxidized oxygenated OA (MO-OOA, also denoted as low-volatility oxygenated organic aerosol in older studies). LO-OOA and MO-OOA are

differentiated by their degree of carbon oxidation. These two factors together account for more than half of total submicron OA (Crippa et al., 2014; Xu et al., 2015a; Jimenez et al., 2009). Despite of their large abundance, the sources of LO-OOA and MO-OOA are unclear and likely vary with location and season. Early studies proposed that LO-OOA is freshly formed SOA from various sources and evolves into MO-OOA with photochemical aging in the atmosphere (Jimenez et al., 2009; Ng et al., 2010). Later, a number of possible sources have been proposed for MO-OOA, including SOA from long-range transport (Hayes et al., 2013; Robinson et al., 2011b), aged biomass burning OA (Bougiatioti et al., 2014; Grieshop et al., 2009), humic-like substances (El Haddad et al., 2013), highly oxygenated molecules (HOMs) formed in the oxidation of monoterpenes (Mutzel et al., 2015; Ehn et al., 2014), and aqueous phase processing (Xu et al., 2016c). Regarding the sources of LO-OOA, Zotter et al. (2014) applied radiocarbon analysis and showed that 68-75% of carbon in LO-OOA in California stems from fossil sources. In the southeastern U.S., Xu et al. (2015a) suggested that the oxidation of biogenic β-pinene by nitrate radicals ($NO_3$) contributes to LO-OOA, though this reaction alone cannot replicate the magnitude of LO-OOA (Pye et al., 2015).

Many different sources of LO-OOA and MO-OOA have been proposed primarily based on comparing the mass spectra between ambient OA factors and laboratory-generated SOA (Jimenez et al., 2009; Kiendler-Scharr et al., 2009; Ng et al., 2010). While the mass spectra comparison approach largely improves our understanding of ambient OA factors, this approach has the following limitations. Firstly, the similarity between two mass spectra is a subjective determination. In other words, a good correlation coefficient (R) value between the mass spectra of an ambient OA factor and a specific type of laboratory SOA does not imply that the laboratory SOA contributes to the specific ambient OA factor. Secondly, such subjectively-defined similarity does not provide quantitative insights into the contribution of SOA from a certain source to a specific OA factor. For example, previous studies have shown that the mass spectrum of laboratory α-pinene SOA is the most similar to that of LO-OOA (Jimenez et al., 2009; Kiendler-Scharr et al., 2009; Ng et al., 2010). However, this similarity neither guarantees that α-pinene SOA is exclusively apportioned into LO-OOA, nor provides information regarding what fraction of α-pinene SOA is apportioned into LO-OOA in ambient environments. Thus, uncertainties associated with the sources of these OA factors still exist. Considering the large abundance of OOA subtypes

and their use as surrogates for ambient SOA, understanding the sources of compounds composing these two OOA subtypes is critical to constrain atmospheric models and SOA budget.

In this study, we integrate lab-in-the-field experiments, extensive ambient ground measurements, and state-of-the-art modeling to improve the understanding of the sources of OA factors and better constrain the OA budget from MT and SQT. Based on lab-in-the-field experiments, we provide objective evidence that newly formed SOA from α-pinene (an important monoterpene) and β-caryophyllene (an important sesquiterpene) is dominantly apportioned to LO-OOA in the southeastern U.S. In addition, we model the SOA concentration from the oxidation of MT and SQT (denoted as $SOA_{MT+SQT}$) and show that $SOA_{MT+SQT}$ reasonably reproduces the magnitude and diurnal variability of LO-OOA measured at multiple sites in the southeastern U.S. Together with other evidence in the literature, we propose that LO-OOA can be used as a measure of $SOA_{MT+SQT}$ in the southeastern U.S. Finally, we discuss how the lab-in-the-field approach allows for the study of SOA formation under realistic atmospheric conditions, which bridges laboratory studies and field measurements and provides a direct way to evaluate the atmospheric relevancy of laboratory studies.

## 2 Method

### 2.1 Lab-in-the-field perturbation experiments

The perturbation experiments were performed in July-August 2016 on the rooftop of the Environmental Science and Technology building on the Georgia Institute of Technology campus. This measurement site is an urban site in Atlanta, Georgia. Multiple ambient field studies have been performed at this site previously (Xu et al., 2015b; Hennigan et al., 2009; Verma et al., 2014). A $2m^3$ Teflon chamber (cubic shape) (Fig. 1) was placed outdoor on the rooftop of the building. The eight corners of the chamber were open (~2”×2”) to the atmosphere to allow for continuous exchange of air with the atmosphere. The perturbation procedure is briefly described below and illustrated in Fig. A1. Firstly, we continuously flushed the chamber with ambient air using two fans, which were placed at two corners of the chamber. During this flushing period, all instruments sampled ambient air and were not connected to the chamber. The flushing period lasted at least 3 hours to ensure that the air composition in the chamber is the same as ambient composition. Secondly, we stopped both fans and connected all instruments to chamber. Because of the continued sampling by the instruments (~20 liter per minute) and the open corners of the chamber,

ambient air continuously entered the chamber, even though the two fans were turned off. Thirdly, after sampling the chamber for about 30min, we injected a known amount of VOC (liquid) into the chamber with a needle, where the liquid vaporized upon injection. We continuously monitored the chamber composition for ~40 min after VOC injection. Lastly, we disconnected all instruments from the chamber, sampled ambient air, and turned on two fans to flush the chamber to prepare for the next perturbation experiment.

Each perturbation experiment can be divided into the following four periods: Amb_Bf (30min ambient measurement period before sampling chamber), Chamber_Bf (from sampling chamber to VOC injection, a period ~30min), Chamber_Af (from VOC injection to stop sampling chamber, a period ~40min), and Amb_Af (30min ambient measurement period after sampling chamber). We perform PMF analysis on the combined ambient and perturbation data and then calculate the changes in the mass concentration of OA factors based on the difference between Chamber_Bf and Chamber_Af, after taking ambient variation into account. The detailed procedure is presented in Appendix A. We develop a comprehensive set of criteria to determine if the changes are statistically significant and if the changes are simply due to ambient variations. The details of these criteria are also discussed in Appendix A.

We perturbed the chamber content by injecting one of the following VOCs: isoprene, α-pinene, β-caryophyllene, *m*-xylene, or naphthalene, which are major biogenic or anthropogenic emissions. We focused on α-pinene and β-caryophyllene, because of their large abundances in their classes and that they are widely studied in the literature (Eddingsaas et al., 2012a; Kurtén et al., 2015; Tasoglou and Pandis, 2015; Ehn et al., 2014; Pathak et al., 2007). For example, α-pinene accounts for about half of monoterpenes emissions (Guenther et al., 2012) and β-caryophyllene is one of the most abundant sesquiterpenes (Helmig et al., 2007). We aim to inject as low of a VOC mixing ratio as possible to be atmospherically relevant. If the injection amount is too large, too much SOA will be produced, which will bias subsequent analysis. We use a needle to inject liquid sample into the chamber. Limited by the needle size, 0.2 μL is selected because it is the minimal amount we could inject with reliable accuracy. The VOC oxidation occurred in ambient air (inside the chamber) and lasted ~40 min. The OA concentration in the chamber after perturbation ranges from 4 to 16 μg $m^{-3}$, which is within the range of typical ambient OA concentrations in the southeastern U.S.

We note that several previous studies have used ambient air (Palm et al., 2017; Leungsakul et al., 2005; Peng et al., 2016), but experimental approaches and purposes of previous studies are different from this study. For example, In Leungsakul et al. (2005), the rural ambient air was used to flush and clean the 270$m^3$ outdoor chamber reactor. After the flushing, both VOCs and oxidants were injected to produce SOA, the concentration of which were orders of magnitude higher than atmospheric levels. In this study, we use ambient air with pre-existing OA in order to examine which factor(s) the fresh SOA from injected VOC are apportioned into by PMF analysis. We aim to produce SOA only from injected VOC, so that an important distinction between our study and pervious work is that we perturbed the ambient air by only VOCs and no additional oxidants are introduced into the chamber.

The perturbation experiments are designed to address some limitations of the mass spectra comparison approach by providing objective and quantitative evaluations. By producing SOA from a known precursor, PMF analysis allows for the apportionment of the newly-formed SOA into various factors without any subjective judgement on the similarity in mass spectra, and provides quantification of the fraction of the newly formed SOA that is apportioned into each factor. The perturbation experiments utilize the actual mixing between ambient OA and newly formed SOA from perturbation, which a standard chamber experiment would not achieve, meaning that the performance of the factorization can be more directly inspected. In addition, as the same instrument set-up is used for both ambient sampling and perturbation experiments, factorization results are free of instrument tuning issues.

## 2.2 Analytical instruments

A suite of analytical instruments was deployed to characterize both the gas-phase and particle-phase compositions. The particle-phase composition was monitored by a scanning mobility particle sizer (SMPS, TSI) and a high resolution time-of-flight aerosol mass spectrometer (HR-ToF-AMS, Aerodyne), which shared the same stainless steel sampling line. A diaphragm pump (flow rate ~8 liter per minute) was connected to this sampling line, which increased the sampling flow rate and reduced particle loss in the sampling line by reducing the residence time in the tubing. The HR-ToF-AMS measures the chemical composition and size distribution of submicron non-refractory species (NR-$PM_1$) with high temporal resolution. The instrument details about HR-ToF-

AMS have been extensively discussed in the literature (Canagaratna et al., 2007; DeCarlo et al., 2006) and the operation of HR-ToF-AMS in this study is described in the section S2 of Supplement.

The gas-phase composition and oxidation products was monitored by an $O_3$ analyzer (Teledyne T400, lower detectable limit 0.6ppb), an ultrasensitive chemiluminescence $NO_x$ monitor (Teledyne 200EU, lower detectable limit 50ppt), and a high-resolution time-of-flight chemical ionization mass spectrometer (HR-ToF-CIMS). The HR-ToF-CIMS with $I^-$ as regent ion can measure a suite of oxygenated volatile organic compounds (oVOCs) at high frequency (1Hz). Detailed working principles and sampling protocol can be found in Lee et al. (2014). The concentrations of VOCs were not measured in this study. All gas-phase measurement instruments shared the same Teflon sampling line. Similar to the particle sampling line, a diaphragm pump (flow rate ~8 liter per minute) was connected to the gas sampling line to reduce the residence time in the tubing.

### 2.3 Positive Matrix Factorization (PMF) analysis

PMF analysis has been widely used for aerosol source apportionment in the atmospheric chemistry community (Jimenez et al., 2009; Crippa et al., 2014; Xu et al., 2015a; Ng et al., 2010; Ulbrich et al., 2009; Beddows et al., 2015; Visser et al., 2015). PMF solves bilinear unmixing factor model by minimizing the summed least squares errors of the fit weighted with the error estimates of each measurement (Paatero and Tapper, 1994; Ulbrich et al., 2009). We utilized the PMF2 solver, which does not require a priori information and reduces subjectivity. In this study, we performed PMF analysis on the high-resolution mass spectra of organic aerosol (inorganic species are excluded) of combined ambient and perturbation data in the one-month measurements. Considering that (1) the perturbation data only account for ~10% of total data and (2) the OA concentration is similar between the perturbation experiments and typical ambient measurements, the perturbation experiments do not create a new factor that does not already exist in the ambient data. This is desirable because it allows PMF analysis to apportion the newly formed OA in the perturbation experiments into pre-existing OA factors in the atmosphere.

We resolved five OA factors, including hydrocarbon-like OA (HOA), cooking OA (COA), isoprene-derived OA (isoprene-OA), less-oxidized oxygenated OA (LO-OOA), and more-oxidized oxygenated OA (MO-OOA). The time series and mass spectra of OA factors are shown in Fig. 2. The same 5 factors have been identified at the same measurement site and extensively

discussed in the literature (Xu et al., 2015a; Xu et al., 2015b; Xu et al., 2017). Below, we only provide a brief description on these OA factors and more details are discussed in section S3 of Supplement. The mass spectrum of HOA is dominated by hydrocarbon-like ions ($C_xH_y^+$ ions) and HOA is a surrogate of primary OA from vehicle emissions (Zhang et al., 2011). For COA, its concentration is higher at meal times and its mass spectrum is characterized by prominent signal at ions $C_3H_5^+$ (*m/z* 41) and $C_4H_7^+$ (*m/z* 55), which likely arise from fatty acids (Huang et al., 2010; Mohr et al., 2009; Allan et al., 2010). The mass spectrum of isoprene-OA is characterized by prominent signal at ions $C_4H_5^+$ (*m/z* 53) and $C_5H_6O^+$ (*m/z* 82) and it is related to the reactive uptake of isoprene oxidation products, isoprene epoxydiols (IEPOX) (Budisulistiorini et al., 2013; Hu et al., 2015; Robinson et al., 2011a; Xu et al., 2015a). LO-OOA and MO-OOA are named based on their differing carbon oxidation state, that is, from -0.70 to -0.34 for LO-OOA and from -0.18 to 0.71 for MO-OOA in the southeastern U.S. (Xu et al., 2015b). We performed 100 bootstrapping runs to quantify the uncertainty of PMF results. As shown in Fig. S1, the statistical uncertainties in the time series and mass spectra of 5 factors are small and the PMF results reported in this study are robust.

### 2.4 Details of multiple ambient sampling sites

Measurements at multiple sites in the southeastern U.S. were performed as part of Southeastern Center for Air Pollution and Epidemiology study (SCAPE) and Southern Oxidant and Aerosol Study (SOAS) in 2012 and 2013. Detailed descriptions about these field studies have been discussed in the literature (Xu et al., 2015a; Xu et al., 2015b) and section S4 of Supplement. The sampling periods are shown in Table S1 and the sampling sites are briefly discussed below.

• Georgia Tech site (GT): This site is located on the rooftop of the Environmental Science and Technology building on the Georgia Institute of Technology (GT) campus, which is about 30-40m above the ground and 840m away from interstate I75/85. This is an urban site in Atlanta. This is also where the perturbation experiments in this study were conducted.

• Jefferson Street site (JST): This is a central SEARCH (SouthEastern Aerosol Research and Characterization) site, which is in Atlanta's urban area with a mixed commercial and residential neighborhood. It is about 2 km west of the GT site. The JST and GT sites are in the same grid cell in CMAQ.

• Yorkville site (YRK): This is a central SEARCH site located in a rural area in Georgia. This site is surrounded by agricultural land and forests and is at about 80 km northwest of JST site.

• Centreville site (CTR): This is a central SEARCH site in rural Alabama. The sampling site is surrounded by forests and away from large urban areas (55km SE and 84 km SW of Tuscaloosa and Birmingham, AL, respectively). The is the main ground site for the SOAS campaign.

### 2.5 Laboratory chamber study on SOA formation from α-pinene

To compare with results from the lab-in-the-field perturbation experiments, we performed laboratory experiments to study the SOA formation from α-pinene photooxidation under different $NO_x$ conditions in the Georgia Tech Environmental Chamber (GTEC) facility. The facility consists of two 12 $m^3$ indoor Teflon chambers, which are suspended inside a temperature-controlled enclosure and surrounded by black lights. The detailed description about chamber facility can be found in Boyd et al. (2015). The experimental procedures have been discussed in Tuet et al. (2017). In brief, the chambers were flushed with clean air prior to each experiment. Then, α-pinene and oxidant sources (i.e., $H_2O_2$, $NO_2$, or HONO) were injected into chamber. Once the concentrations of species stabilize, the black lights were turned on to initiate photooxidation. The experimental conditions are summarized in Table S2. Considering that the OA mass concentration affects the partitioning of semi-volatile organic compounds (Odum et al., 1996) and hence affects the organic mass spectra measured by AMS, we calculated the average mass spectra in these laboratory studies by only using the data when the OA mass concentration is below 10 μg $m^{-3}$, which is similar to that in our ambient perturbation experiments.

### 2.6 Community Multiscale Air Quality (CMAQ) Model

To test the hypothesis that a large fraction of LO-OOA originates from monoterpenes and sesquiterpenes in the southeastern U.S., we used the Community Multiscale Air Quality (CMAQ) atmospheric chemical transport model to simulate the SOA from monoterpenes and sesquiterpenes ($SOA_{MT+SQT}$) in the southeastern U.S. and then compared the simulated $SOA_{MT+SQT}$ with measured LO-OOA. CMAQ v5.2gamma was run over the continental U.S. for time periods between May 2012 to July 2013 with 12km × 12km horizontal resolution. We focus our analysis on the southeastern U.S., which comprises 11 states (Arkansas, Alabama, Florida, Georgia, Kentucky, Louisiana, Mississippi, North Carolina, South Carolina, Tennessee, and Virginia). The meteorological inputs were generated with version 3.8 of the Weather Research and Forecasting

model (WRF), Advanced Research WRF (ARW) core. We also applied lightning assimilation to improve convective rainfall (Heath et al., 2016). Anthropogenic emissions were based on the EPA (Environmental Protection Agency) NEI (National Emission Inventory) 2011 v2. Biogenic emissions were predicted by the BEIS (Biogenic Emission Inventory System) v3.6.1. The gas-phase chemistry was based on CB6r3 (Carbon Bond v6.3).

We performed two simulations with different organic aerosol treatment. The "default simulation" generally follows the scheme of Carlton et al. (2010), with the addition of IEPOX SOA following Pye et al. (2013) and documented in Appel et al. (2017) (Fig. S2a). The traditional two-product absorptive partitioning scheme (Odum et al., 1996) is used in "default simulation" to describe SOA formation from monoterpenes using data from laboratory experiments by Griffin et al. (1999). In the "updated simulation", we incorporate two recent findings. Firstly, we implemented MT+$NO_3$ chemistry to explicitly account for the organic nitrate compounds that have recently been shown to be a ubiquitous and important component of OA (Pye et al., 2015; Kiendler-Scharr et al., 2016; Lee et al., 2016; Ng et al., 2017). We follow the scheme described in Pye et al. (2015) to represent the formation and partition of organic nitrates from monoterpenes via multiple reaction pathways (i.e., oxidation by $NO_3$ and oxidation by $OH/O_3$ followed by $RO_2$+NO). Secondly, we improved the parameterization of SOA formation from MT+$O_3$/OH based on a recent study by Saha and Grieshop (2016), who applied a dual-thermodenuder system to study the α-pinene ozonolysis SOA. The authors extracted parameters (i.e., SOA yields and enthalpies of evaporation) by using an evaporation-kinetics model and volatility basis set (VBS). The SOA yields in Saha and Grieshop (2016) are consistent with recent findings on the formation of HOMs (Ehn et al., 2014; Zhang et al., 2015) and help to explain the observed slow evaporation of α-pinene SOA (Vaden et al., 2011). In the updated simulation, we use the VBS framework with parameters derived from Saha and Grieshop (2016). The new parameterization allows for enthalpies of vaporization that are more consistent with species of the specified volatility. The properties of the volatility bins in the VBS framework are listed in Table S3. A schematic of SOA treatment in "updated simulation" is shown in Fig. S2b. In the following discussions, we focus on the results from "updated simulation". The comparison between "default simulation" and "updated simulation" can be found in the section S5 of Supplement.

## 3 Results and Discussions

### 3.1 α-pinene perturbation experiments

A total of 19 α-pinene perturbation experiments were performed at different times of the day (i.e., from 9am to 9pm) to probe a wide range of reaction conditions. The injection time and concentrations of $O_3$ and $NO_x$ during α-pinene perturbation experiments are summarized in Table S4. Based on the chamber volume and injected liquid α-pinene volume (0.2 μL), initially ~14 ppb α-pinene is injected into chamber. Due to lack of VOC measurements, we build a box model to simulate the fate of α-pinene in the chamber (section S6 of Supplement). We estimate that roughly 10% of α-pinene is reacted in the chamber and most of α-pinene is carried out of the chamber due to dilution with ambient air.

Fig. 3 shows the time series of OA factors in a typical α-pinene perturbation experiment. An evident burst and increase of LO-OOA after α-pinene injection occurs. This provides direct evidence that freshly formed α-pinene SOA contributes to LO-OOA. About 15 min after α-pinene injection, LO-OOA concentration starts to decrease, as ambient air continuously flows into the chamber and dilutes the concentration of LO-OOA (section S6 of Supplement). As shown in Fig. S3, the major known gas-phase oxidation products of α-pinene measured by HR-ToF-CIMS (Eddingsaas et al., 2012b; Lee et al., 2016; Yu et al., 1999) show an immediate increase after α-pinene injection. This verifies the rapid oxidation of α-pinene in the chamber.

Fig. 4a shows the perturbation-induced changes in the concentrations of OA factors for all α-pinene experiments. Out of 19 experiments, the LO-OOA concentration is enhanced in 14 experiments. Also, among all OA factors, LO-OOA shows the largest enhancement. This directly supports that freshly formed α-pinene SOA contributes to LO-OOA. The enhancement in LO-OOA concentration differs between experiments, mainly because the perturbations were performed at different times of day (i.e., from 9am to 9pm) and with different reaction variables (i.e., temperature, relative humidity, oxidants concentrations, $NO_x$, etc). Despite the large difference in reaction conditions, we note that both LO-OOA enhancement amount and LO-OOA formation rate (i.e., slope of LO-OOA increase) correlate positively with ozone concentration (Fig. 5). This correlation suggests that the concentration of oxidants, both ozone and hydroxy radical (OH, which is not measured in this study but is known to positively correlate with ozone in the atmosphere), plays a more controlling role in the amount of OA formed in α-pinene experiment

than other reaction variables do. This is likely because higher oxidant concentrations lead to more α-pinene consumption and hence more OA production with the same reaction time.

MO-OOA only increases in 1 out of 19 α-pinene experiments. The highly oxygenated molecules (HOMs), which are rapidly produced from the oxidation of α-pinene, are a hypothesized source of MO-OOA, because of the high O:C ratio of HOMs (Ehn et al., 2014; Mutzel et al., 2015). However, HOMs are first generation monoterpene products co-formed with semivolatile SOA species, and the lack of enhancement in MO-OOA suggests that the HOMs are unlikely contributors to MO-OOA. We cannot rule out the possibilities that HOMs are not formed under our experimental conditions, and future studies on the simultaneous verification of HOMs formation and apportion of HOMs by PMF analysis are warranted.

Isoprene-derived OA (isoprene-OA) increases in 7 out of 19 α-pinene experiments. This increase is surprising because the isoprene-OA factor (also referred to as "IEPOX-OA" in some studies) is typically interpreted as SOA from the reactive uptake of IEPOX, but our results suggest that the isoprene-OA factor could have interferences from α-pinene SOA. The isoprene-OA enhancement is due to interference from newly formed α-pinene SOA, rather than that the injected α-pinene affecting the oxidation of pre-existing isoprene or affecting the gas/particle partitioning of pre-existing semi-volatile species in the chamber, because of the following reasons. Firstly, based on $I^-$ HR-ToF-CIMS measurement, the concentration of isoprene oxidation products, such as IEPOX+ISOPOOH ($C_5H_{10}O_3 \bullet I^-$) and isoprene hydroxyl nitrates ($C_5H_9NO_4 \bullet I^-$), did not change after α-pinene injection (Fig. S3b). In addition, after injecting α-pinene, the increase in SOA concentration is less than 4 μg $m^{-3}$, which does not substantially perturb the gas/particle partition of pre-existing semi-volatile species. Finally, the time series of isoprene-OA and LO-OOA in the same α-pinene perturbation experiment is strongly correlated (Fig. S4a). It is well studied that isoprene produces SOA slower than α-pinene, as isoprene SOA involves higher-generation products. If the enhancement in isoprene-OA factor is due to isoprene oxidation, the enhancement of isoprene-OA is expected to occur later than the enhancement of LO-OOA, but it is not observed in the experiments. Thus, the strong correlation between isoprene-OA and LO-OOA in the same α-pinene perturbation experiment serves as another evidence that the enhancement in isoprene-OA factor is due to interference from newly formed α-pinene SOA, rather than oxidation of isoprene after injecting α-pinene.

The interference of α-pinene SOA on isoprene-OA factor helps to address some uncertainties regarding the isoprene-OA factor in the literature. For example, Liu et al. (2015) compared the mass spectrum of laboratory-derived IEPOX SOA with isoprene-OA factors at some sites. The authors observed stronger correlation for isoprene-OA factors resolved at Borneo (Robinson et al., 2011a) and Amazon (Chen et al., 2015), and weaker correlation at Atlanta, U.S. (Budisulistiorini et al., 2013) and Ontario, Canada (Slowik et al., 2011). As another example, the fraction of measured total IEPOX SOA molecular tracers in isoprene-OA factor highly varies with location, ranging from 26% at Look Rock, TN (Budisulistiorini et al., 2015) to 78% at Centreville, AL (Hu et al., 2015). To address the uncertainties in the above two examples, one possible reason is that the isoprene-OA factors resolved at different sites are not purely from IEPOX uptake. Isoprene-OA factors likely have interference from monoterpenes SOA or other sources, but the interference magnitude varies with locations.

While the perturbation experiments clearly point out the possibility that isoprene-OA factor could have interference from α-pinene SOA, three caveats should be kept in mind. First, in this study, the enhancement magnitude of isoprene-OA is ~20% of that of LO-OOA (Fig. S5a), but this interference magnitude would vary with locations and seasons. Second, the perturbation experiments simulate a period with increasing α-pinene SOA concentration. The applicability of the conclusions drawn from this specific scenario to general atmosphere with more dynamic variations of OA sources warrants further exploration. Third, the perturbation experiments are conducted at ground level, whereas evidence from aircraft studies suggests that production of isoprene SOA may be stronger at the top of the boundary layer (Allan et al., 2014).

Primary OA factors, i.e., HOA and COA, only show slight increases in 1 or 2 α-pinene experiments, indicating a lack of interference from α-pinene SOA in these factors.

### 3.2 β-caryophyllene perturbation experiments

A total of 6 β-caryophyllene perturbation experiments were performed. 0.2 μL β-caryophyllene is injected into the chamber, corresponding to a mixing ratio of 10 ppb. The concentrations of $O_3$ and $NO_x$ during β-caryophyllene perturbation experiments are summarized in Table S4. In all β-caryophyllene perturbation experiments, LO-OOA also shows a significant enhancement (Fig. 4b). This clearly shows that the freshly formed SOA from β-caryophyllene oxidation can be another source of LO-OOA. In addition to LO-OOA, COA shows an unexpected increase in 5 out of 6 β-

caryophyllene experiments. We have ample evidence that the COA factor at the measurement site has contributions from cooking activities. Firstly, the diurnal variation of COA peaks during meal times (Fig. S6a). Additionally, the COA concentration shows clear increase on football days, consistent with barbecue activities on campus and close to the measurement site. Finally, the COA concentration is enhanced on the days right before the start of a new semester when there are many fraternity/sorority rush events (i.e., barbecue activities) on campus (Fig. S6b and S6c). However, the COA enhancement in β-caryophyllene experiments underscores the fact that COA may not be purely from cooking activities in areas with large biogenic emissions.

### 3.3 Perturbation experiments with other VOCs

In addition to α-pinene and β-caryophyllene, we also performed a few perturbation experiments by injecting isoprene, *m*-xylene, or naphthalene. However, the SOA formation from these VOCs is not detectable. This is mainly due to either lower SOA yields (of isoprene) or slower oxidation rates (of *m*-xylene and naphthalene) compared to α-pinene and β-caryophyllene, which are discussed in section S6 of Supplement.

We have also performed four perturbation experiments by injecting acidic sulfate particles to probe reactive uptake of IEPOX. We observed enhancement in isoprene-OA concentration after the injection of sulfate particles. The detailed results are included in Appendix B.

### 3.4 LO-OOA as a surrogate of $SOA_{MT+SQT}$ in the Southeastern U.S.

We propose that the major source of LO-OOA in the southeastern U.S. is the fresh SOA from oxidation of MT and SQT by various oxidants ($O_3$, OH, and $NO_3$), based on multiple lines of evidence. First, the southeastern U.S. is characterized by large biogenic emissions, including monoterpenes and sesquiterpenes (Guenther et al., 2012). Second, the majority of carbon in SOA is modern in the southeastern U.S. Weber et al. (2007) measured that the biogenic fraction of SOA is roughly 70-80% at two urban sites in Georgia that were also used in our study. We note that measurements in Weber et al. (2007) were performed in 2004 and the biogenic fraction of SOA is expected to be higher in 2016 than 2004, as a result of reductions in anthropogenic emissions (Blanchard et al., 2010). Third, previous studies suggest that the oxidation of β-pinene (another important monoterpene) by nitrate radicals ($NO_3$) contributes to LO-OOA in the southeastern U.S. (Boyd et al., 2015; Xu et al., 2015a), though this reaction alone cannot replicate the magnitude of LO-OOA (Pye et al., 2015). Fourth, the mass spectra of LO-OOA are almost identical (i.e., R

ranges from 0.95 to 0.99 in Fig. S7) across all the seven datasets in our study. In addition, LO-OOA across all datasets also shares the same diurnal trends (Xu et al., 2015a). The similarity in LO-OOA features suggests that LO-OOA generally share similar sources across multiple sites and in different seasons in the southeastern U.S. Fifth, the lab-in-the-field perturbation experiments provide objective evidence that the majority of freshly formed SOA from the oxidation of MT and SQT contributes to LO-OOA. Sixthly, using the updated CMAQ model (i.e., explicit organic nitrates and Saha and Grieshop (2016) VBS for MT+$O_3$/OH SOA), we found that the simulated $SOA_{MT+SQT}$ reasonably reproduces both the magnitude and diurnal variability of LO-OOA for all sites (Fig. 6a). The model bias is within ~20% for most sites, except for Centreville, Alabama (i.e., 43% for CTR_June dataset). Fig. 6b present maps of ground-level $SOA_{MT+SQT}$ concentration corresponding to the time periods of observational data, and the $SOA_{MT+SQT}$ concentration is substantially higher in the southeast than other U.S. regions. While, the $SOA_{MT+SQT}$ is present throughout the year, it reaches the largest concentration in summer. The spatial and seasonal variation of $SOA_{MT+SQT}$ concentration is consistent with MT and SQT emissions (Guenther et al., 2012). The consistency between modeled $SOA_{MT+SQT}$ and measured LO-OOA at multiple sites and in different seasons builds confidence in our hypothesis that LO-OOA largely arises from the oxidation of MT and SQT in the southeastern U.S.

We note that we do not conclude that LO-OOA arises exclusively from MT and SQT. SOA from other precursors or other pathways may contribute to LO-OOA, but the related contributions are expected to be much smaller than MT and SQT in the southeastern U.S. Firstly, the contributions of anthropogenic SOA to LO-OOA are likely small. The emissions of anthropogenic VOCs are much weaker than that of biogenic VOCs in the southeastern U.S. (Goldstein et al., 2009). We modeled that the concentration of anthropogenic SOA is on the order of 0.1 $\mu g\ m^{-3}$ for our datasets (Fig. S8). Even if we double the SOA yields of anthropogenic VOCs to account for the potential vapor wall loss in laboratory studies (Zhang et al., 2014), the concentration of SOA from anthropogenic VOCs oxidation is still negligible compared to $SOA_{MT+SQT}$. The low modeled concentration of anthropogenic SOA is consistent with Zhang et al. (2018), who showed that the measured tracers of anthropogenic SOA only account for 2% of total OA in Centreville, AL. Secondly, other reaction pathways, like aqueous-phase chemistry or some unexplored reaction, may contribute to LO-OOA. However, the consistency between modeled $SOA_{MT+SQT}$ and LO-OOA suggests that LO-OOA can be reasonably represented by a model based on current

knowledge. In addition, SOA produced from aqueous-phase chemistry is generally highly oxidized (Lee et al., 2011) and may be apportioned into MO-OOA, instead of LO-OOA. A recent study by Xu et al. (2016c) suggests that aqueous-phase SOA is a major source of MO-OOA in China.

We limit our hypothesis that major source of LO-OOA is the oxidation of MT and SQT to the southeastern U.S. The southeastern US is a unique location in that there have been a large number of field studies in recent years at multiple locations and seasons throughout the region. Results from these studies provided additional constraints for OA sources in this region (Carlton et al., 2018; Zhang et al., 2018; Xu et al., 2015a; Warneke et al., 2016). At other locations, there is evidence that LO-OOA factor represents different sources. For example, radiocarbon analysis shows that 68-75% of carbon in LO-OOA in California stems from fossil sources (Hayes et al., 2013; Zotter et al., 2014), suggesting the contribution from anthropogenic SOA to LO-OOA. Also, in the wintertime of many locations, LO-OOA and MO-OOA are not separated and a single OOA factor is resolved (Xu et al., 2016b; Lanz et al., 2008). Further developments are needed if one were to use the perturbation experimental approach for source apportionments of OA at other sites, if auxiliary constraints from field measurements/lab studies/modeling are not readily available for those sites.

### 3.5 Connection between laboratory and field studies

Due to the difficulties associated with accurately measuring complex chemical processes in the atmosphere, laboratory studies have been an integral part in our understanding of atmospheric chemistry (Burkholder et al., 2017). However, the representativeness of laboratory studies under simplified conditions with respect to the complex atmosphere is difficult to evaluate. One unique feature of our lab-in-the-field approach is that the VOC oxidation and SOA formation proceed under realistic atmospheric conditions. Taking advantage of this, we provide a direct link between laboratory studies and ambient observations. Previous laboratory studies have shown that NO can affect SOA composition by influencing the fate of organic peroxy radical ($RO_2$, a critical radical intermediate formed from VOC oxidation) (Kroll and Seinfeld, 2008; Sarrafzadeh et al., 2016; Presto et al., 2005). To evaluate the representativeness of laboratory studies and investigate the effects of NO on SOA composition, in Fig. 7, we compare the chemical composition of α-pinene SOA formed in laboratory studies under different NO conditions (denoted as $SOA_{lab}$) with those in α-pinene ambient perturbation experiments (denoted as $SOA_{ambient}$). The degree of similarity in

OA mass spectra (i.e., evaluated by the correlation coefficient) between laboratory α-pinene SOA generated under NO-free condition (i.e., denoted as $SOA_{lab,NO\text{-}free}$, using $H_2O_2$ photolysis as oxidant source) and $SOA_{ambient}$ shows a strong dependence on ambient NO concentration, under which the $SOA_{ambient}$ is formed. The degree of similarity in mass spectra decreases rapidly when ambient NO increases from 0.1 to 0.2ppb, and then reaches a plateau at ~0.3ppb NO. The opposite trend is observed when laboratory α-pinene SOA generated in the presence of high NO concentrations (i.e., denoted as $SOA_{lab,high\text{-}NO}$, using the photolysis of $NO_2$ or nitrous acid as oxidant source) are compared with $SOA_{ambient}$. These observations show the transition of $RO_2$ fate as a function of NO under ambient conditions. For the perturbation experiments performed when ambient NO is below ~0.1ppb, the mass spectra of $SOA_{ambient}$ are similar to $SOA_{lab,NO\text{-}free}$, consistent with that $RO_2$ mainly reacts with hydroperoxyl ($HO_2$) or isomerizes. In contrast, for the perturbation experiments performed when ambient NO is above ~0.3ppb, the mass spectra of $SOA_{ambient}$ are similar to $SOA_{lab,high\text{-}NO}$, consistent with that the $RO_2$ fate is dominated by NO. This NO level (~0.3ppb) is consistent with the NO level required to dominate the fate of $RO_2$ in the atmosphere, as calculated by using previously measured $HO_2$ and kinetic rate constants (section S8 of Supplement). These observations also illustrate that the SOA composition from laboratory studies can be representative of atmosphere. We note that the mass spectra of $SOA_{ambient}$ are generally more similar with that of laboratory SOA generated using $NO_2$ photolysis as oxidant source than using nitrous acid photolysis. This suggests that laboratory experiments using $NO_2$ photolysis as oxidant source better represent ambient high NO oxidation conditions in the southeastern U.S. than experiments using nitrous acid do. Possible explanations are discussed in section S7 of Supplement. This finding provides new insights into designing future laboratory experiments to better mimic the oxidations in ambient environments.

## 4 Implications

In this study, we performed lab-in-the-field perturbation experiments and provided objective evidence that the majority of fresh SOA from the oxidation of MT and SQT contributes to LO-OOA. Based on multiple lines of evidence, we propose that LO-OOA can be used as a surrogate of fresh SOA from MT and SQT in the southeastern U.S. We showed that modeled $SOA_{MT+SQT}$ could reasonably reproduce both the magnitude and diurnal variability of LO-OOA at different sites and in different seasons. Based on the model simulation, we estimate that the annual concentration of $SOA_{MT+SQT}$ in $PM_{2.5}$ in the southeastern U.S. is ~2 μg $m^{-3}$ (i.e., average

concentration over the six sampling periods and over the southeastern U.S. in the updated simulation). This accounts for 20% of World Health Organization $PM_{2.5}$ guideline (i.e., 10 μg $m^{-3}$ annual mean) and indicates a significant contributor of environmental risk to the 77 million habitants in the southeastern U.S. Also, the estimated abundance of $SOA_{MT+SQT}$ is substantially larger than represented in current models (Lane et al., 2008; Zheng et al., 2015), but in line with the conclusion from Zhang et al. (2018). Zhang et al. (2018) used a different methodology, characterization of molecular tracers of MT SOA at Centreville, AL (a site included in our study as well), to conclude that monoterpenes are the largest source of summertime organic aerosol in the southeastern United States. The oxidation of MT and SQT is likely an under-estimated contributor to PM in the present day and perhaps during the pre-industrial period, which determines the baseline state of atmosphere and the estimate of climate forcing by anthropogenic emissions (Carslaw et al., 2013). Models need to improve the description of the MT and SQT oxidation to reduce the uncertainties in estimated OA budget and subsequent climate forcing.

Using LO-OOA as a surrogate of $SOA_{MT+SQT}$ in the southeastern U.S., our ambient ground measurements suggest that at least 19-34% of OA in the southeastern U.S. is from the oxidation of biogenic monoterpenes and sesquiterpenes (Xu et al., 2015a). The fraction of biogenic OA in the southeastern U.S. is even larger if we consider that isoprene-OA could account for 21-36% of OA in summer (albeit potential interferences of SOA from monoterpenes oxidation) and that MO-OOA (24-49% of OA) likely contains SOA from long-term photochemical oxidation of biogenic VOCs. The dominant biogenic origin of SOA poses a challenge to control its burden in the southeastern U.S., if the roles of anthropogenic oxidants and other controlling factors are not recognized. Previous studies have shown that the SOA formation from biogenic VOCs can be mediated by anthropogenic emissions, such as nitrogen oxides and sulfur dioxide (Hoyle et al., 2011; Goldstein et al., 2009; Surratt et al., 2010; Rollins et al., 2012; Xu et al., 2015a). Thus, regulating anthropogenic emissions could help reduce SOA concentration (Lane et al., 2008; Pye et al., 2015; Zheng et al., 2015). For example, as observed in our ambient perturbation experiments, one controlling parameter of α-pinene SOA formation is the concentration of atmospheric oxidants ($O_3$, OH, and $NO_3$), which are known to strongly depend on $NO_x$ concentration. As it has been shown that anthropogenic emissions exert complex and non-linear influences on biogenic SOA formation (Zheng et al., 2015), the effectiveness of regulating anthropogenic emissions on biogenic SOA burden requires careful investigations.

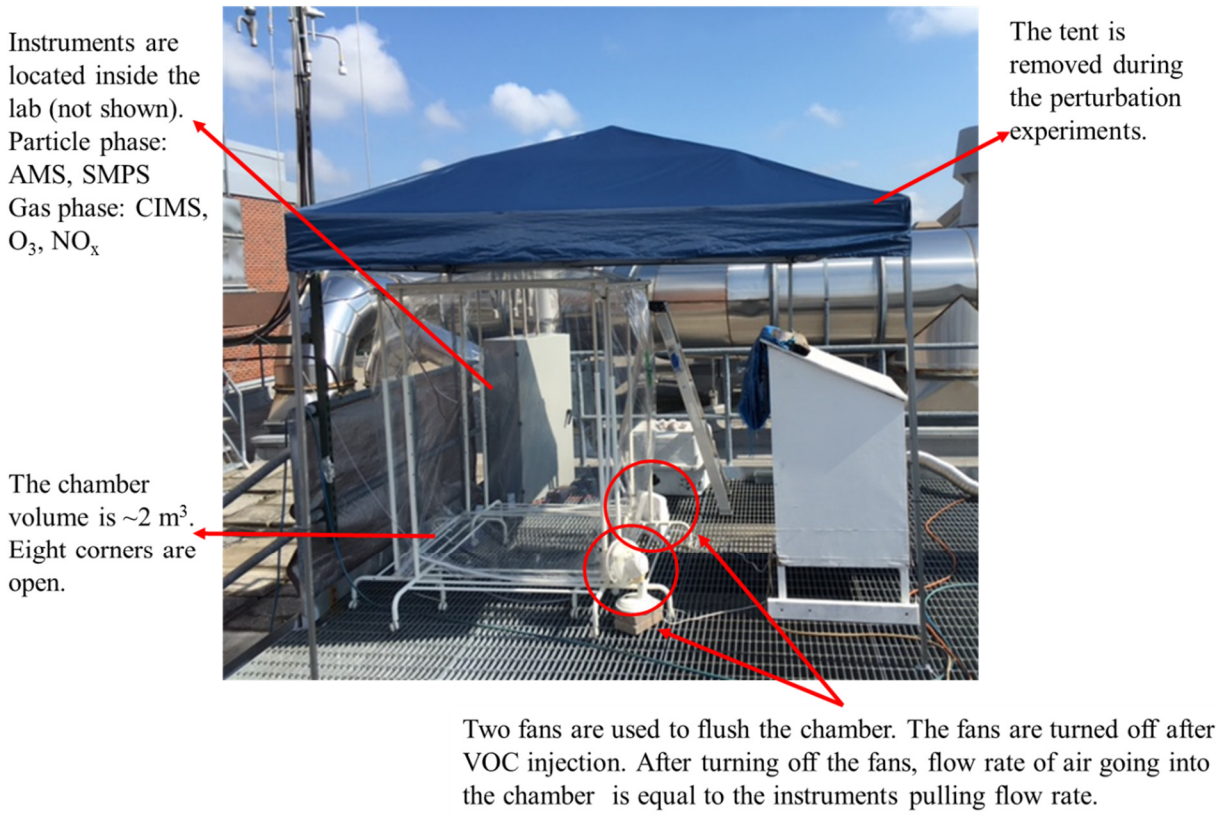


544

545 Fig. 1. The instrument setup for ambient perturbation experiments.

546

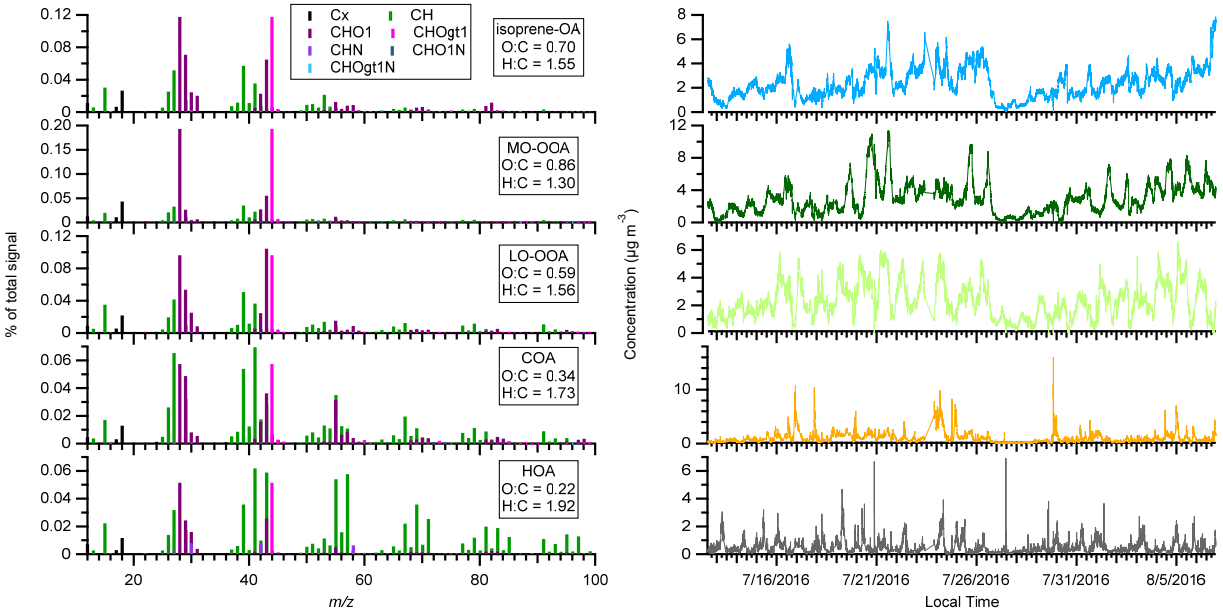


547

548 Fig. 2. The mass spectra and time series of OA factors in perturbation study. The time series
549 includes both the ambient data and perturbation experiments data.

550

551

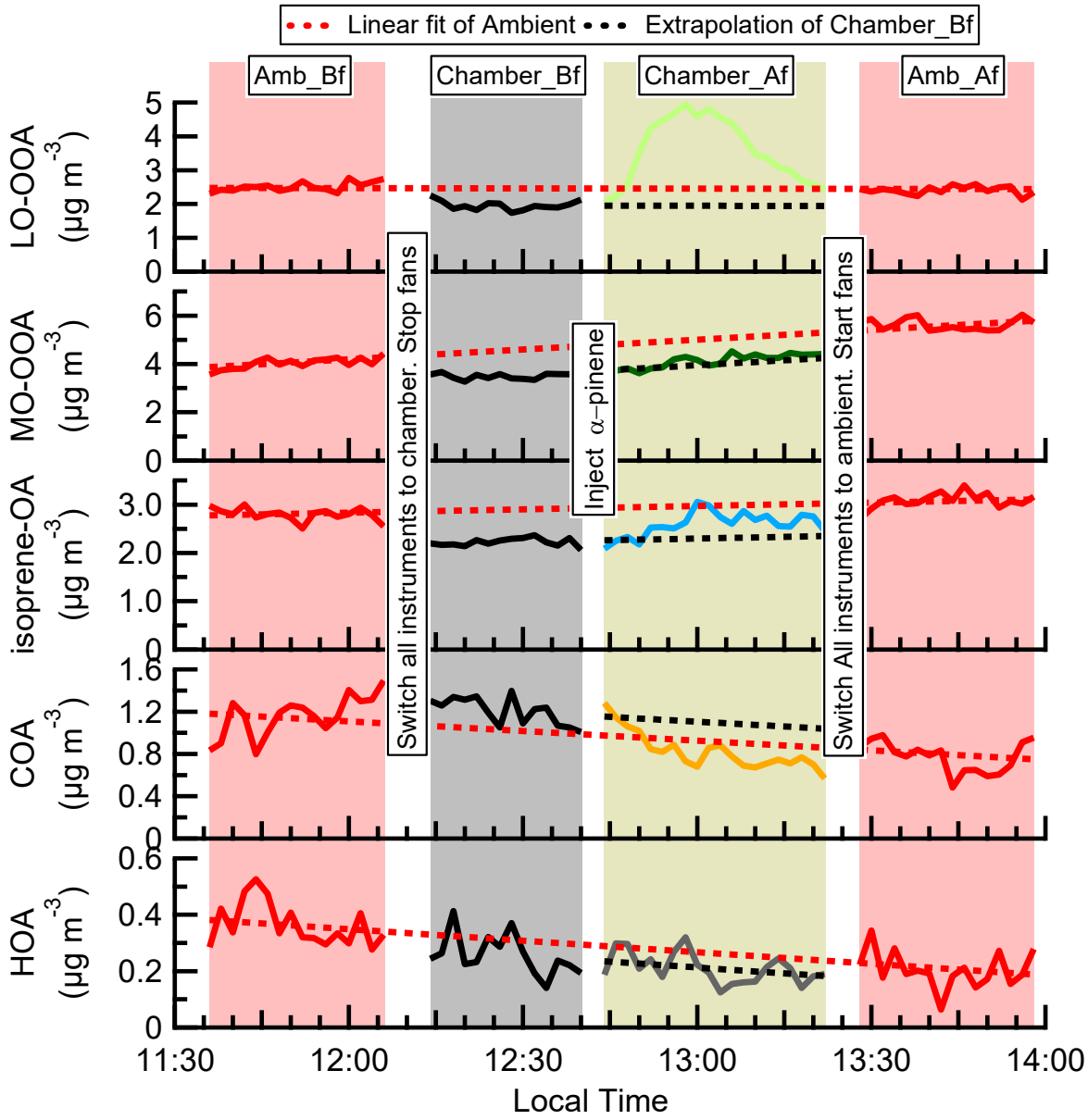


552

553 Fig. 3. The time series of OA factors in an α-pinene perturbation experiment (Expt ID: ap_0801_1).
554 Each perturbation experiment includes four periods: Amb_Bf (~30min), Chamber_Bf (~30min),
555 Chamber_Af (~40min), and Amb_Af (~40min). "Amb" and "Chamber" represent that instruments
556 are sampling ambient and chamber, respectively. "Bf" and "Af" stand for before and after
557 perturbation, respectively. The solid lines are measurement data. The dashed red lines are the linear
558 fits of ambient data (i.e., combined Amb_Bf and Amb_Af). The slopes are used to extrapolate
559 Chamber_Bf data to Chamber_Af period (i.e., dashed black lines). The validity of the linearity
560 assumption is discussed in Appendix A. The difference between measurements (i.e., solid lines)
561 and extrapolated Chamber_Bf (i.e., dashed black lines) represents the change caused by
562 perturbation.

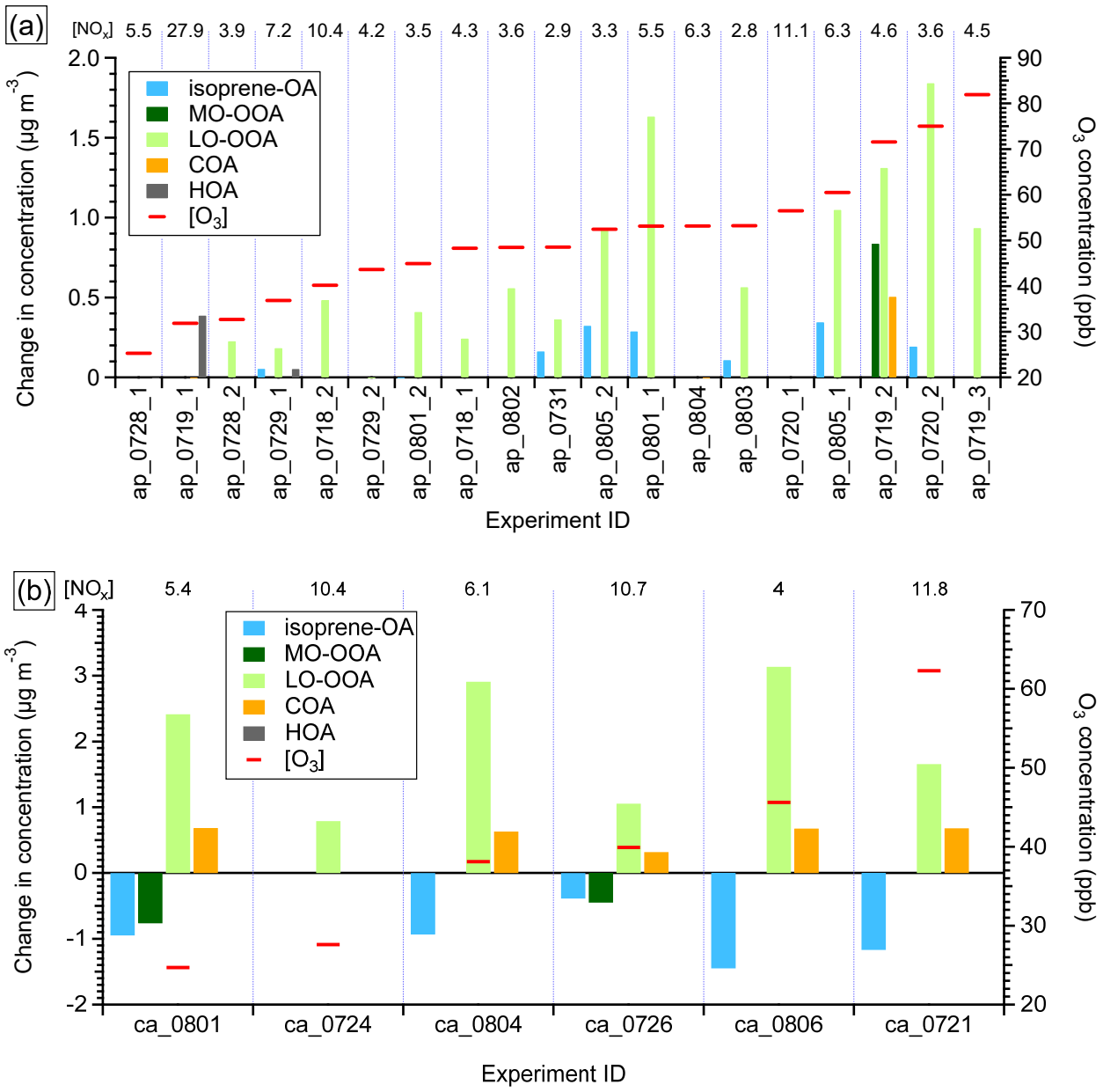


Fig. 4. The statistically significant changes in the concentrations of OA factors after perturbation by (a) α-pinene and (b) β-caryophyllene. The experiments are sorted by average [$O_3$] during Chamber_Af. The average [$NO_x$] during Chamber_Af are shown on top of the figure. The changes in concentration are the differences between measurements during Chamber_Af and extrapolated Chamber_Bf (Appendix A). A set of criteria are developed to evaluate if the changes are statistically significant and if the changes are due to ambient variation (Appendix A). Isoprene-OA decreases after β-caryophyllene injection. The reason for this decrease is unclear, but likely due to the limitations of PMF analysis, which assumes constant mass spectra of OA factors over time (section S3 of Supplement).

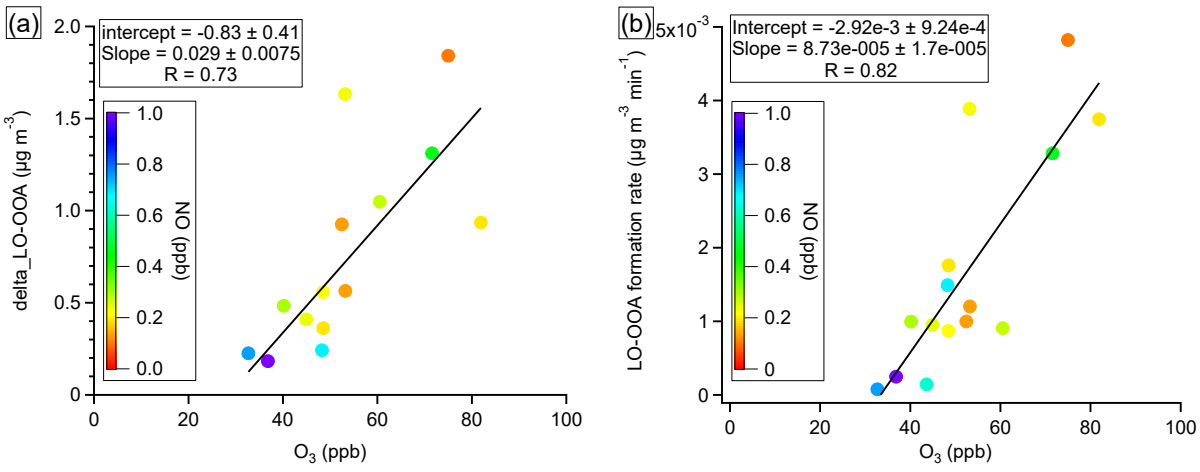


574

575 Fig. 5. Observations of trends in (a) LO-OOA enhancement amount and (b) LO-OOA formation
576 rate with $O_3$ concentration in α-pinene perturbation experiments. The data points are colored by
577 average NO concentration during Chamber_Af period. The slopes, intercepts, and correlation
578 coefficients (R) are obtained by least square fit.

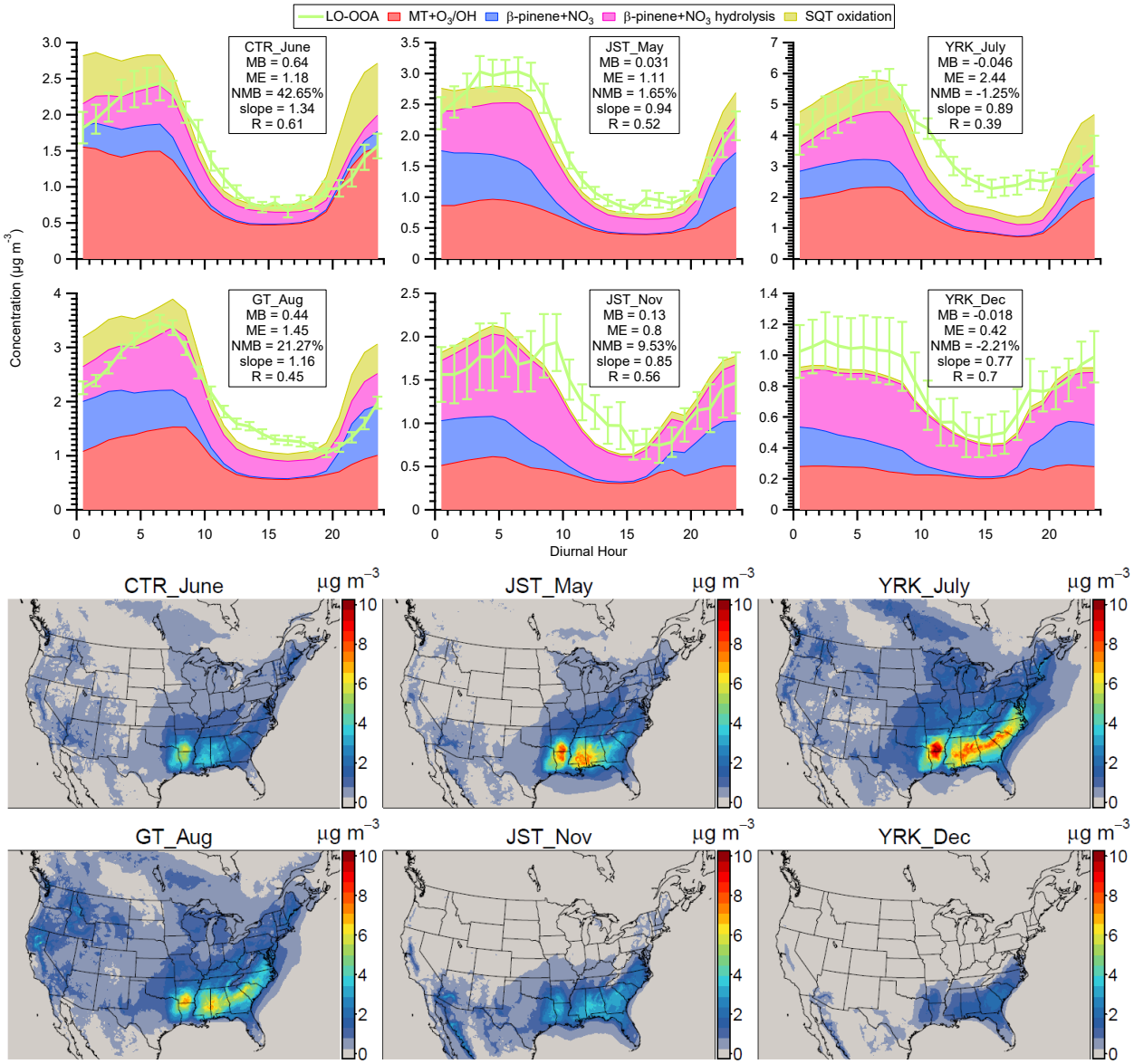


Fig. 6. (a) top panel: the diurnal trends of LO-OOA and modeled SOA from monoterpenes and sesquiterpenes ($SOA_{MT+SQT}$) at different sampling sites in the southeastern U.S. (b) bottom panel: maps of modeled ground-level $SOA_{MT+SQT}$ concentration coinciding with the time periods of intensive ambient sampling. Model results shown here are from the updated simulation. Abbreviations correspond to Centreville (CTR), Jefferson Street (JST), Yorkville (YRK), Georgia Institute of Technology (GT). Detailed sampling periods are shown in Table S1. In panel (a), since the perturbation experiments show that 16% of SOA from α-pinene oxidation is apportioned into isoprene-OA (Fig. S5a), we only include 84% of modeled SOA from $MT+O_3/OH$ when comparing with LO-OOA for the sites with isoprene-OA. The mean bias (MB), mean error (ME), and normalized mean bias (NMB) for each site are shown in each panel. The slopes and correlation coefficients (R) are obtained by least square fit. The error bars indicate the standard error. In panel (b), average $SOA_{MT+SQT}$ concentration in $PM_{2.5}$ during each sampling period is reported.

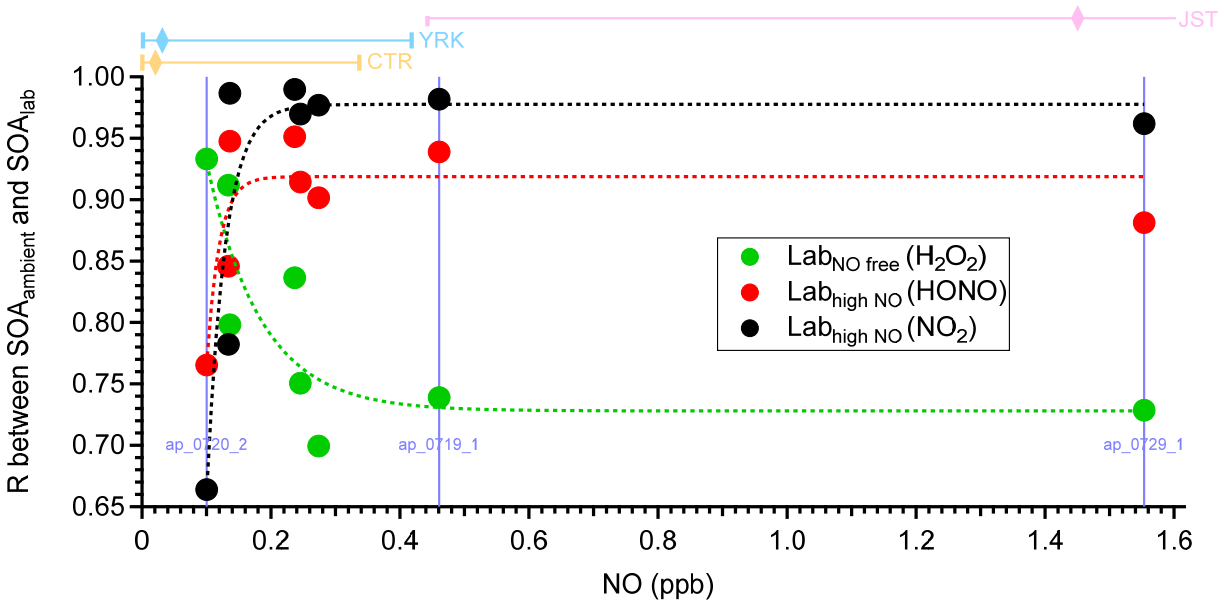


Fig. 7. The correlation coefficients between the mass spectra of OA formed in laboratory under different NO conditions ("$SOA_{lab}$") and those of OA formed in ambient α-pinene perturbation experiments ("$SOA_{ambient}$"). The subscripts "lab" and "ambient" indicate the SOA formed under laboratory conditions and ambient conditions, respectively. Three different oxidant sources (i.e., $H_2O_2$, HONO, and $NO_2$) are used to create different NO concentrations in laboratory studies. The mass spectra of "$SOA_{ambient}$" are calculated by comparing the mass spectra of OA during Chamber_Af and those of extrapolated Chamber_Bf (section S7 of Supplement). To calculate reliable mass spectra of "$SOA_{ambient}$", only the experiments with significant OA enhancement are analyzed and shown here (Appendix A). The x-axis is the average NO concentration during each perturbation experiment. The data points on the same vertical line (i.e., the same NO concentration) are from the same perturbation experiment, but compared to three different laboratory experiments. The dashed lines are used to guide eyes. The bars on top of the figure represent the $10^{th}$, $50^{th}$, and $90^{th}$ percentiles of NO concentration for CTR (Centreville, AL), YRK (Yorkville, GA), and JST (Jefferson Street, GA) in 2013. The NO concentration is measured by the SouthEastern Aerosol Research and Characterization (SEARCH) network. The $90^{th}$ percentile of NO concentration in JST is 14.8 ppb, which is not shown in the figure.

**Acknowledgments**

L.X. and N.L.N. acknowledged support from US Environmental Protection Agency (EPA) STAR Grant RD-83540301, and National Science Foundation (NSF) grants 1555034 and 1455588. The HR-ToF-CIMS was purchased with NSF Major Research Instrumentation (MRI) grant 1428738. HOTP contributions were supported by a Presidential Early Career Award for Scientists and Engineers (PECASE). The authors thank R. J. Weber and M. R. Canagaratna for helpful discussions, the SEARCH personnel for their many contributions, the CSRA for preparing emissions and meteorology for CMAQ simulations. The US EPA through its Office of Research and Development supported the research described here. It has been subjected to Agency administrative review and approved for publication but may not necessarily reflect official Agency policy.

## References


Allan, J. D., Williams, P. I., Morgan, W. T., Martin, C. L., Flynn, M. J., Lee, J., Nemitz, E., Phillips, G. J., Gallagher, M. W., and Coe, H.: Contributions from transport, solid fuel burning and cooking to primary organic aerosols in two UK cities, Atmos. Chem. Phys., 10, 647-668, 10.5194/acp-10-647-2010, 2010.

Allan, J. D., Morgan, W. T., Darbyshire, E., Flynn, M. J., Williams, P. I., Oram, D. E., Artaxo, P., Brito, J., Lee, J. D., and Coe, H.: Airborne observations of IEPOX-derived isoprene SOA in the Amazon during SAMBBA, Atmos. Chem. Phys., 14, 11393-11407, 10.5194/acp-14-11393-2014, 2014.

Appel, K. W., Napelenok, S. L., Foley, K. M., Pye, H. O. T., Hogrefe, C., Luecken, D. J., Bash, J. O., Roselle, S. J., Pleim, J. E., Foroutan, H., Hutzell, W. T., Pouliot, G. A., Sarwar, G., Fahey, K. M., Gantt, B., Gilliam, R. C., Heath, N. K., Kang, D., Mathur, R., Schwede, D. B., Spero, T. L., Wong, D. C., and Young, J. O.: Description and evaluation of the Community Multiscale Air Quality (CMAQ) modeling system version 5.1, Geosci. Model Dev., 10, 1703-1732, 10.5194/gmd-10-1703-2017, 2017.

Beddows, D. C. S., Harrison, R. M., Green, D. C., and Fuller, G. W.: Receptor modelling of both particle composition and size distribution from a background site in London, UK, Atmos. Chem. Phys., 15, 10107-10125, 10.5194/acp-15-10107-2015, 2015.

Blanchard, C. L., Hidy, G. M., Tanenbaum, S., Rasmussen, R., Watkins, R., and Edgerton, E.: NMOC, ozone, and organic aerosol in the southeastern United States, 1999-2007 1 Spatial and temporal variations of NMOC concentrations and composition in Atlanta, Georgia, Atmospheric Environment, 44, 4827-4839, DOI 10.1016/j.atmosenv.2010.08.036, 2010.

Bougiatioti, A., Stavroulas, I., Kostenidou, E., Zarmpas, P., Theodosi, C., Kouvarakis, G., Canonaco, F., Prévôt, A. S. H., Nenes, A., Pandis, S. N., and Mihalopoulos, N.: Processing of biomass-burning aerosol in the eastern Mediterranean during summertime, Atmos. Chem. Phys., 14, 4793-4807, 10.5194/acp-14-4793-2014, 2014.

Boyd, C. M., Sanchez, J., Xu, L., Eugene, A. J., Nah, T., Tuet, W. Y., Guzman, M. I., and Ng, N. L.: Secondary organic aerosol formation from the β-pinene+NO3 system: effect of humidity and peroxy radical fate, Atmos. Chem. Phys., 15, 7497-7522, 10.5194/acp-15-7497-2015, 2015.

Budisulistiorini, S. H., Canagaratna, M. R., Croteau, P. L., Marth, W. J., Baumann, K., Edgerton, E. S., Shaw, S. L., Knipping, E. M., Worsnop, D. R., Jayne, J. T., Gold, A., and Surratt, J. D.: Real-Time Continuous Characterization of Secondary Organic Aerosol Derived from Isoprene Epoxydiols in Downtown Atlanta, Georgia, Using the Aerodyne Aerosol Chemical Speciation Monitor, Environ Sci Technol, 47, 5686-5694, Doi 10.1021/Es400023n, 2013.

Budisulistiorini, S. H., Li, X., Bairai, S. T., Renfro, J., Liu, Y., Liu, Y. J., McKinney, K. A., Martin, S. T., McNeill, V. F., Pye, H. O. T., Nenes, A., Neff, M. E., Stone, E. A., Mueller, S., Knote, C., Shaw, S. L., Zhang, Z., Gold, A., and Surratt, J. D.: Examining the effects of anthropogenic emissions on isoprene-derived secondary organic aerosol formation during the 2013 Southern Oxidant and Aerosol Study (SOAS) at the Look Rock, Tennessee ground site, Atmos. Chem. Phys., 15, 8871-8888, 10.5194/acp-15-8871-2015, 2015.

Burkholder, J. B., Abbatt, J. P. D., Barnes, I., Roberts, J. M., Melamed, M. L., Ammann, M., Bertram, A. K., Cappa, C. D., Carlton, A. M. G., Carpenter, L. J., Crowley, J. N., Dubowski, Y., George, C., Heard, D. E., Herrmann, H., Keutsch, F. N., Kroll, J. H., McNeill, V. F., Ng, N. L., Nizkorodov, S. A., Orlando, J. J., Percival, C. J., Picquet-Varrault, B., Rudich, Y., Seakins, P. W., Surratt, J. D., Tanimoto, H., Thornton, J. A., Zhu, T., Tyndall, G. S., Wahner, A., Weschler, C. J., Wilson, K. R., and Ziemann, P. J.: The Essential Role for Laboratory Studies in Atmospheric Chemistry, Environ Sci Technol, 10.1021/acs.est.6b04947, 2017.

Canagaratna, M. R., Jayne, J. T., Jimenez, J. L., Allan, J. D., Alfarra, M. R., Zhang, Q., Onasch, T. B., Drewnick, F., Coe, H., Middlebrook, A., Delia, A., Williams, L. R., Trimborn, A. M., Northway, M. J., DeCarlo, P. F., Kolb, C. E., Davidovits, P., and Worsnop, D. R.: Chemical and microphysical characterization of ambient aerosols with the aerodyne aerosol mass spectrometer, Mass Spectrometry Reviews, 26, 185-222, 10.1002/mas.20115, 2007.

Canonaco, F., Crippa, M., Slowik, J. G., Baltensperger, U., and Prévôt, A. S. H.: SoFi, an IGOR-based interface for the efficient use of the generalized multilinear engine (ME-2) for the source apportionment: ME-2 application to aerosol mass spectrometer data, Atmos. Meas. Tech., 6, 3649-3661, 10.5194/amt-6-3649-2013, 2013.

Carlton, A. G., Bhave, P. V., Napelenok, S. L., Edney, E. O., Sarwar, G., Pinder, R. W., Pouliot, G. A., and Houyoux, M.: Model Representation of Secondary Organic Aerosol in CMAQv4.7, Environ Sci Technol, 44, 8553-8560, 10.1021/es100636q, 2010.

Carlton, A. G., Gouw, J. d., Jimenez, J. L., Ambrose, J. L., Attwood, A. R., Brown, S., Baker, K. R., Brock, C., Cohen, R. C., Edgerton, S., Farkas, C. M., Farmer, D., Goldstein, A. H., Gratz, L., Guenther, A., Hunt, S., Jaeglé, L., Jaffe, D. A., Mak, J., McClure, C., Nenes, A., Nguyen, T. K., Pierce, J. R., Sa, S. d., Selin, N. E., Shah, V., Shaw, S., Shepson, P. B., Song, S., Stutz, J., Surratt, J. D., Turpin, B. J., Warneke, C., Washenfelder, R. A., Wennberg, P. O., and Zhou, X.: Synthesis of the Southeast Atmosphere Studies: Investigating Fundamental Atmospheric Chemistry Questions, B Am Meteorol Soc, 99, 547-567, 10.1175/bams-d-16-0048.1, 2018.

Carslaw, K. S., Lee, L. A., Reddington, C. L., Pringle, K. J., Rap, A., Forster, P. M., Mann, G. W., Spracklen, D. V., Woodhouse, M. T., Regayre, L. A., and Pierce, J. R.: Large contribution of natural aerosols to uncertainty in indirect forcing, Nature, 503, 67-71, Doi 10.1038/Nature12674, 2013.

709 Chen, Q., Farmer, D. K., Rizzo, L. V., Pauliquevis, T., Kuwata, M., Karl, T. G., Guenther, A.,
710 Allan, J. D., Coe, H., Andreae, M. O., Pöschl, U., Jimenez, J. L., Artaxo, P., and Martin, S. T.:
711 Submicron particle mass concentrations and sources in the Amazonian wet season (AMAZE-08),
712 Atmos. Chem. Phys., 15, 3687-3701, 10.5194/acp-15-3687-2015, 2015.
713
714 Crippa, M., Canonaco, F., Lanz, V. A., Äijälä, M., Allan, J. D., Carbone, S., Capes, G., Ceburnis,
715 D., Dall'Osto, M., Day, D. A., DeCarlo, P. F., Ehn, M., Eriksson, A., Freney, E., Hildebrandt Ruiz,
716 L., Hillamo, R., Jimenez, J. L., Junninen, H., Kiendler-Scharr, A., Kortelainen, A. M., Kulmala,
717 M., Laaksonen, A., Mensah, A. A., Mohr, C., Nemitz, E., O'Dowd, C., Ovadnevaite, J., Pandis, S.
718 N., Petäjä, T., Poulain, L., Saarikoski, S., Sellegri, K., Swietlicki, E., Tiitta, P., Worsnop, D. R.,
719 Baltensperger, U., and Prévôt, A. S. H.: Organic aerosol components derived from 25 AMS data
720 sets across Europe using a consistent ME-2 based source apportionment approach, Atmos. Chem.
721 Phys., 14, 6159-6176, 10.5194/acp-14-6159-2014, 2014.
722
723 DeCarlo, P. F., Kimmel, J. R., Trimborn, A., Northway, M. J., Jayne, J. T., Aiken, A. C., Gonin,
724 M., Fuhrer, K., Horvath, T., Docherty, K. S., Worsnop, D. R., and Jimenez, J. L.: Field-Deployable,
725 High-Resolution, Time-of-Flight Aerosol Mass Spectrometer, Anal Chem, 78, 8281-8289,
726 10.1021/ac061249n, 2006.
727
728 Eddingsaas, N. C., Loza, C. L., Yee, L. D., Chan, M., Schilling, K. A., Chhabra, P. S., Seinfeld, J.
729 H., and Wennberg, P. O.: α-pinene photooxidation under controlled chemical conditions –
730 Part 2: SOA yield and composition in low- and high-NOx environments, Atmos. Chem. Phys., 12,
731 7413-7427, 10.5194/acp-12-7413-2012, 2012a.
732
733 Eddingsaas, N. C., Loza, C. L., Yee, L. D., Seinfeld, J. H., and Wennberg, P. O.: α-pinene
734 photooxidation under controlled chemical conditions – Part 1: Gas-phase composition in low- and
735 high-NO<sub>x</sub> environments, Atmos. Chem. Phys., 12, 6489-6504, 10.5194/acp-12-
736 6489-2012, 2012b.
737
738 Ehn, M., Thornton, J. A., Kleist, E., Sipila, M., Junninen, H., Pullinen, I., Springer, M., Rubach,
739 F., Tillmann, R., Lee, B., Lopez-Hilfiker, F., Andres, S., Acir, I.-H., Rissanen, M., Jokinen, T.,
740 Schobesberger, S., Kangasluoma, J., Kontkanen, J., Nieminen, T., Kurten, T., Nielsen, L. B.,
741 Jorgensen, S., Kjaergaard, H. G., Canagaratna, M., Maso, M. D., Berndt, T., Petaja, T., Wahner,
742 A., Kerminen, V.-M., Kulmala, M., Worsnop, D. R., Wildt, J., and Mentel, T. F.: A large source
743 of low-volatility secondary organic aerosol, Nature, 506, 476-479, 10.1038/nature13032, 2014.
744
745 El Haddad, I., D'Anna, B., Temime-Roussel, B., Nicolas, M., Boreave, A., Favez, O., Voisin, D.,
746 Sciare, J., George, C., Jaffrezo, J. L., Wortham, H., and Marchand, N.: Towards a better
747 understanding of the origins, chemical composition and aging of oxygenated organic aerosols: case
748 study of a Mediterranean industrialized environment, Marseille, Atmos. Chem. Phys., 13, 7875-
749 7894, 10.5194/acp-13-7875-2013, 2013.
750

751 Goldstein, A. H., Koven, C. D., Heald, C. L., and Fung, I. Y.: Biogenic carbon and anthropogenic
752 pollutants combine to form a cooling haze over the southeastern United States, Proceedings of the
753 National Academy of Sciences, 106, 8835-8840, 10.1073/pnas.0904128106, 2009.
754
755 Grieshop, A. P., Donahue, N. M., and Robinson, A. L.: Laboratory investigation of photochemical
756 oxidation of organic aerosol from wood fires 2: analysis of aerosol mass spectrometer data, Atmos.
757 Chem. Phys., 9, 2227-2240, 10.5194/acp-9-2227-2009, 2009.
758
759 Griffin, R. J., Cocker, D. R., Flagan, R. C., and Seinfeld, J. H.: Organic aerosol formation from
760 the oxidation of biogenic hydrocarbons, J Geophys Res-Atmos, 104, 3555-3567, Doi
761 10.1029/1998jd100049, 1999.
762
763 Guenther, A., Jiang, X., Heald, C. L., Sakulyanontvittaya, T., Duhl, T., Emmons, L. K., and Wang,
764 X.: The Model of Emissions of Gases and Aerosols from Nature version 2.1 (MEGAN2.1): an
765 extended and updated framework for modeling biogenic emissions, Geosci. Model Dev., 5, 1471-
766 1492, 10.5194/gmd-5-1471-2012, 2012.
767
768 Hallquist, M., Wenger, J. C., Baltensperger, U., Rudich, Y., Simpson, D., Claeys, M., Dommen,
769 J., Donahue, N. M., George, C., Goldstein, A. H., Hamilton, J. F., Herrmann, H., Hoffmann, T.,
770 Iinuma, Y., Jang, M., Jenkin, M. E., Jimenez, J. L., Kiendler-Scharr, A., Maenhaut, W., McFiggans,
771 G., Mentel, T. F., Monod, A., Prevot, A. S. H., Seinfeld, J. H., Surratt, J. D., Szmigielski, R., and
772 Wildt, J.: The formation, properties and impact of secondary organic aerosol: current and emerging
773 issues, Atmos Chem Phys, 9, 5155-5236, 2009.
774
775 Hayes, P. L., Ortega, A. M., Cubison, M. J., Froyd, K. D., Zhao, Y., Cliff, S. S., Hu, W. W.,
776 Toohey, D. W., Flynn, J. H., Lefer, B. L., Grossberg, N., Alvarez, S., Rappenglueck, B., Taylor, J.
777 W., Allan, J. D., Holloway, J. S., Gilman, J. B., Kuster, W. C., De Gouw, J. A., Massoli, P., Zhang,
778 X., Liu, J., Weber, R. J., Corrigan, A. L., Russell, L. M., Isaacman, G., Worton, D. R., Kreisberg,
779 N. M., Goldstein, A. H., Thalman, R., Waxman, E. M., Volkamer, R., Lin, Y. H., Surratt, J. D.,
780 Kleindienst, T. E., Offenberg, J. H., Dusanter, S., Griffith, S., Stevens, P. S., Brioude, J., Angevine,
781 W. M., and Jimenez, J. L.: Organic aerosol composition and sources in Pasadena, California,
782 during the 2010 CalNex campaign, J Geophys Res-Atmos, 118, 9233-9257, Doi
783 10.1002/Jgrd.50530, 2013.
784
785 Heath, N. K., Pleim, J. E., Gilliam, R. C., and Kang, D.: A simple lightning assimilation technique
786 for improving retrospective WRF simulations, Journal of Advances in Modeling Earth Systems, 8,
787 1806-1824, 10.1002/2016MS000735, 2016.
788
789 Helmig, D., Ortega, J., Duhl, T., Tanner, D., Guenther, A., Harley, P., Wiedinmyer, C., Milford,
790 J., and Sakulyanontvittaya, T.: Sesquiterpene Emissions from Pine Trees − Identifications,
791 Emission Rates and Flux Estimates for the Contiguous United States, Environ Sci Technol, 41,
792 1545-1553, 10.1021/es0618907, 2007.
793

794 Hennigan, C. J., Bergin, M. H., Russell, A. G., Nenes, A., and Weber, R. J.: Gas/particle
795 partitioning of water-soluble organic aerosol in Atlanta, Atmos Chem Phys, 9, 3613-3628, 2009.
796
797 Hodzic, A., Kasibhatla, P. S., Jo, D. S., Cappa, C. D., Jimenez, J. L., Madronich, S., and Park, R.
798 J.: Rethinking the global secondary organic aerosol (SOA) budget: stronger production, faster
799 removal, shorter lifetime, Atmos. Chem. Phys., 16, 7917-7941, 10.5194/acp-16-7917-2016, 2016.
800
801 Hoyle, C. R., Boy, M., Donahue, N. M., Fry, J. L., Glasius, M., Guenther, A., Hallar, A. G., Hartz,
802 K. H., Petters, M. D., Petaja, T., Rosenoern, T., and Sullivan, A. P.: A review of the anthropogenic
803 influence on biogenic secondary organic aerosol, Atmos Chem Phys, 11, 321-343, DOI
804 10.5194/acp-11-321-2011, 2011.
805
806 Hu, W. W., Campuzano-Jost, P., Palm, B. B., Day, D. A., Ortega, A. M., Hayes, P. L., Krechmer,
807 J. E., Chen, Q., Kuwata, M., Liu, Y. J., de Sá, S. S., McKinney, K., Martin, S. T., Hu, M.,
808 Budisulistiorini, S. H., Riva, M., Surratt, J. D., St. Clair, J. M., Isaacman-Van Wertz, G., Yee, L.
809 D., Goldstein, A. H., Carbone, S., Brito, J., Artaxo, P., de Gouw, J. A., Koss, A., Wisthaler, A.,
810 Mikoviny, T., Karl, T., Kaser, L., Jud, W., Hansel, A., Docherty, K. S., Alexander, M. L., Robinson,
811 N. H., Coe, H., Allan, J. D., Canagaratna, M. R., Paulot, F., and Jimenez, J. L.: Characterization
812 of a real-time tracer for isoprene epoxydiols-derived secondary organic aerosol (IEPOX-SOA)
813 from aerosol mass spectrometer measurements, Atmos. Chem. Phys., 15, 11807-11833,
814 10.5194/acp-15-11807-2015, 2015.
815
816 Huang, X. F., He, L. Y., Hu, M., Canagaratna, M. R., Sun, Y., Zhang, Q., Zhu, T., Xue, L., Zeng,
817 L. W., Liu, X. G., Zhang, Y. H., Jayne, J. T., Ng, N. L., and Worsnop, D. R.: Highly time-resolved
818 chemical characterization of atmospheric submicron particles during 2008 Beijing Olympic
819 Games using an Aerodyne High-Resolution Aerosol Mass Spectrometer, Atmos Chem Phys, 10,
820 8933-8945, DOI 10.5194/acp-10-8933-2010, 2010.
821
822 Jimenez, J. L., Canagaratna, M. R., Donahue, N. M., Prevot, A. S. H., Zhang, Q., Kroll, J. H.,
823 DeCarlo, P. F., Allan, J. D., Coe, H., Ng, N. L., Aiken, A. C., Docherty, K. S., Ulbrich, I. M.,
824 Grieshop, A. P., Robinson, A. L., Duplissy, J., Smith, J. D., Wilson, K. R., Lanz, V. A., Hueglin,
825 C., Sun, Y. L., Tian, J., Laaksonen, A., Raatikainen, T., Rautiainen, J., Vaattovaara, P., Ehn, M.,
826 Kulmala, M., Tomlinson, J. M., Collins, D. R., Cubison, M. J., Dunlea, E. J., Huffman, J. A.,
827 Onasch, T. B., Alfarra, M. R., Williams, P. I., Bower, K., Kondo, Y., Schneider, J., Drewnick, F.,
828 Borrmann, S., Weimer, S., Demerjian, K., Salcedo, D., Cottrell, L., Griffin, R., Takami, A.,
829 Miyoshi, T., Hatakeyama, S., Shimono, A., Sun, J. Y., Zhang, Y. M., Dzepina, K., Kimmel, J. R.,
830 Sueper, D., Jayne, J. T., Herndon, S. C., Trimborn, A. M., Williams, L. R., Wood, E. C.,
831 Middlebrook, A. M., Kolb, C. E., Baltensperger, U., and Worsnop, D. R.: Evolution of Organic
832 Aerosols in the Atmosphere, Science, 326, 1525-1529, DOI 10.1126/science.1180353, 2009.
833
834 Kiendler-Scharr, A., Zhang, Q., Hohaus, T., Kleist, E., Mensah, A., Mentel, T. F., Spindler, C.,
835 Uerlings, R., Tillmann, R., and Wildt, J.: Aerosol Mass Spectrometric Features of Biogenic SOA:
836 Observations from a Plant Chamber and in Rural Atmospheric Environments, Environ Sci Technol,
837 43, 8166-8172, 10.1021/es901420b, 2009.

Kiendler-Scharr, A., Mensah, A. A., Friese, E., Topping, D., Nemitz, E., Prevot, A. S. H., Äijälä, M., Allan, J., Canonaco, F., Canagaratna, M., Carbone, S., Crippa, M., Dall Osto, M., Day, D. A., De Carlo, P., Di Marco, C. F., Elbern, H., Eriksson, A., Freney, E., Hao, L., Herrmann, H., Hildebrandt, L., Hillamo, R., Jimenez, J. L., Laaksonen, A., McFiggans, G., Mohr, C., O'Dowd, C., Otjes, R., Ovadnevaite, J., Pandis, S. N., Poulain, L., Schlag, P., Sellegri, K., Swietlicki, E., Tiitta, P., Vermeulen, A., Wahner, A., Worsnop, D., and Wu, H. C.: Ubiquity of organic nitrates from nighttime chemistry in the European submicron aerosol, Geophysical Research Letters, 43, 7735-7744, 10.1002/2016GL069239, 2016.

Kroll, J. H., Ng, N. L., Murphy, S. M., Varutbangkul, V., Flagan, R. C., and Seinfeld, J. H.: Chamber studies of secondary organic aerosol growth by reactive uptake of simple carbonyl compounds, J Geophys Res-Atmos, 110, Doi 10.1029/2005jd006004, 2005.

Kroll, J. H., and Seinfeld, J. H.: Chemistry of secondary organic aerosol: Formation and evolution of low-volatility organics in the atmosphere, Atmospheric Environment, 42, 3593-3624, DOI 10.1016/j.atmosenv.2008.01.003, 2008.

Kurtén, T., Rissanen, M. P., Mackeprang, K., Thornton, J. A., Hyttinen, N., Jørgensen, S., Ehn, M., and Kjaergaard, H. G.: Computational Study of Hydrogen Shifts and Ring-Opening Mechanisms in α-Pinene Ozonolysis Products, The Journal of Physical Chemistry A, 119, 11366-11375, 10.1021/acs.jpca.5b08948, 2015.

Lane, T. E., Donahue, N. M., and Pandis, S. N.: Effect of NOx on Secondary Organic Aerosol Concentrations, Environ Sci Technol, 42, 6022-6027, 10.1021/es703225a, 2008.

Lanz, V. A., Alfarra, M. R., Baltensperger, U., Buchmann, B., Hueglin, C., Szidat, S., Wehrli, M. N., Wacker, L., Weimer, S., Caseiro, A., Puxbaum, H., and Prevot, A. S. H.: Source Attribution of Submicron Organic Aerosols during Wintertime Inversions by Advanced Factor Analysis of Aerosol Mass Spectra, Environ Sci Technol, 42, 214-220, 10.1021/es0707207, 2008.

Lee, A. K. Y., Herckes, P., Leaitch, W. R., Macdonald, A. M., and Abbatt, J. P. D.: Aqueous OH oxidation of ambient organic aerosol and cloud water organics: Formation of highly oxidized products, Geophysical Research Letters, 38, n/a-n/a, 10.1029/2011GL047439, 2011.

Lee, B. H., Lopez-Hilfiker, F. D., Mohr, C., Kurtén, T., Worsnop, D. R., and Thornton, J. A.: An Iodide-Adduct High-Resolution Time-of-Flight Chemical-Ionization Mass Spectrometer: Application to Atmospheric Inorganic and Organic Compounds, Environ Sci Technol, 48, 6309-6317, 10.1021/es500362a, 2014.

Lee, B. H., Mohr, C., Lopez-Hilfiker, F. D., Lutz, A., Hallquist, M., Lee, L., Romer, P., Cohen, R. C., Iyer, S., Kurtén, T., Hu, W., Day, D. A., Campuzano-Jost, P., Jimenez, J. L., Xu, L., Ng, N. L., Guo, H., Weber, R. J., Wild, R. J., Brown, S. S., Koss, A., de Gouw, J., Olson, K., Goldstein, A.

H., Seco, R., Kim, S., McAvey, K., Shepson, P. B., Starn, T., Baumann, K., Edgerton, E. S., Liu, J., Shilling, J. E., Miller, D. O., Brune, W., Schobesberger, S., D'Ambro, E. L., and Thornton, J. A.: Highly functionalized organic nitrates in the southeast United States: Contribution to secondary organic aerosol and reactive nitrogen budgets, Proceedings of the National Academy of Sciences, 113, 1516-1521, 10.1073/pnas.1508108113, 2016.

Lelieveld, J., Evans, J. S., Fnais, M., Giannadaki, D., and Pozzer, A.: The contribution of outdoor air pollution sources to premature mortality on a global scale, Nature, 525, 367-371, 10.1038/nature15371, 2015.

Leungsakul, S., Jeffries, H. E., and Kamens, R. M.: A kinetic mechanism for predicting secondary aerosol formation from the reactions of d-limonene in the presence of oxides of nitrogen and natural sunlight, Atmospheric Environment, 39, 7063-7082, https://doi.org/10.1016/j.atmosenv.2005.08.024, 2005.

Liu, Y., Kuwata, M., Strick, B. F., Geiger, F. M., Thomson, R. J., McKinney, K. A., and Martin, S. T.: Uptake of Epoxydiol Isomers Accounts for Half of the Particle-Phase Material Produced from Isoprene Photooxidation via the HO2 Pathway, Environ Sci Technol, 49, 250-258, 10.1021/es5034298, 2015.

Liu, Y., Kuwata, M., McKinney, K. A., and Martin, S. T.: Uptake and release of gaseous species accompanying the reactions of isoprene photo-oxidation products with sulfate particles, Phys Chem Chem Phys, 18, 1595-1600, 10.1039/C5CP04551G, 2016.

Mohr, C., Huffman, J. A., Cubison, M. J., Aiken, A. C., Docherty, K. S., Kimmel, J. R., Ulbrich, I. M., Hannigan, M., and Jimenez, J. L.: Characterization of Primary Organic Aerosol Emissions from Meat Cooking, Trash Burning, and Motor Vehicles with High-Resolution Aerosol Mass Spectrometry and Comparison with Ambient and Chamber Observations, Environ Sci Technol, 43, 2443-2449, 10.1021/es8011518, 2009.

Mutzel, A., Poulain, L., Berndt, T., Iinuma, Y., Rodigast, M., Böge, O., Richters, S., Spindler, G., Sipilä, M., Jokinen, T., Kulmala, M., and Herrmann, H.: Highly Oxidized Multifunctional Organic Compounds Observed in Tropospheric Particles: A Field and Laboratory Study, Environ Sci Technol, 10.1021/acs.est.5b00885, 2015.

Ng, N. L., Canagaratna, M. R., Zhang, Q., Jimenez, J. L., Tian, J., Ulbrich, I. M., Kroll, J. H., Docherty, K. S., Chhabra, P. S., Bahreini, R., Murphy, S. M., Seinfeld, J. H., Hildebrandt, L., Donahue, N. M., DeCarlo, P. F., Lanz, V. A., Prevot, A. S. H., Dinar, E., Rudich, Y., and Worsnop, D. R.: Organic aerosol components observed in Northern Hemispheric datasets from Aerosol Mass Spectrometry, Atmos Chem Phys, 10, 4625-4641, DOI 10.5194/acp-10-4625-2010, 2010.

Ng, N. L., Brown, S. S., Archibald, A. T., Atlas, E., Cohen, R. C., Crowley, J. N., Day, D. A., Donahue, N. M., Fry, J. L., Fuchs, H., Griffin, R. J., Guzman, M. I., Herrmann, H., Hodzic, A.,

924 Iinuma, Y., Jimenez, J. L., Kiendler-Scharr, A., Lee, B. H., Luecken, D. J., Mao, J., McLaren, R.,
925 Mutzel, A., Osthoff, H. D., Ouyang, B., Picquet-Varrault, B., Platt, U., Pye, H. O. T., Rudich, Y.,
926 Schwantes, R. H., Shiraiwa, M., Stutz, J., Thornton, J. A., Tilgner, A., Williams, B. J., and Zaveri,
927 R. A.: Nitrate radicals and biogenic volatile organic compounds: oxidation, mechanisms, and
928 organic aerosol, Atmos. Chem. Phys., 17, 2103-2162, 10.5194/acp-17-2103-2017, 2017.
929
930 Odum, J. R., Hoffmann, T., Bowman, F., Collins, D., Flagan, R. C., and Seinfeld, J. H.:
931 Gas/Particle Partitioning and Secondary Organic Aerosol Yields, Environ Sci Technol, 30, 2580-
932 2585, 10.1021/es950943+, 1996.
933
934 Paatero, P., and Tapper, U.: Positive Matrix Factorization - a Nonnegative Factor Model with
935 Optimal Utilization of Error-Estimates of Data Values, Environmetrics, 5, 111-126, DOI
936 10.1002/env.3170050203, 1994.
937
938 Paatero, P.: The Multilinear Engine—A Table-Driven, Least Squares Program for Solving
939 Multilinear Problems, Including the n-Way Parallel Factor Analysis Model, Journal of
940 Computational and Graphical Statistics, 8, 854-888, 10.1080/10618600.1999.10474853, 1999.
941
942 Palm, B. B., de Sá, S. S., Day, D. A., Campuzano-Jost, P., Hu, W., Seco, R., Sjostedt, S. J., Park,
943 J. H., Guenther, A. B., Kim, S., Brito, J., Wurm, F., Artaxo, P., Thalman, R., Wang, J., Yee, L. D.,
944 Wernis, R., Isaacman-VanWertz, G., Goldstein, A. H., Liu, Y., Springston, S. R., Souza, R.,
945 Newburn, M. K., Alexander, M. L., Martin, S. T., and Jimenez, J. L.: Secondary organic aerosol
946 formation from ambient air in an oxidation flow reactor in central Amazonia, Atmos. Chem. Phys.
947 Discuss., 2017, 1-56, 10.5194/acp-2017-795, 2017.
948
949 Palm, B. B., de Sá, S. S., Day, D. A., Campuzano-Jost, P., Hu, W., Seco, R., Sjostedt, S. J., Park,
950 J. H., Guenther, A. B., Kim, S., Brito, J., Wurm, F., Artaxo, P., Thalman, R., Wang, J., Yee, L. D.,
951 Wernis, R., Isaacman-VanWertz, G., Goldstein, A. H., Liu, Y., Springston, S. R., Souza, R.,
952 Newburn, M. K., Alexander, M. L., Martin, S. T., and Jimenez, J. L.: Secondary organic aerosol
953 formation from ambient air in an oxidation flow reactor in central Amazonia, Atmos. Chem. Phys.,
954 18, 467-493, 10.5194/acp-18-467-2018, 2018.
955
956 Pathak, R. K., Stanier, C. O., Donahue, N. M., and Pandis, S. N.: Ozonolysis of alpha-pinene at
957 atmospherically relevant concentrations: Temperature dependence of aerosol mass fractions
958 (yields), J Geophys Res-Atmos, 112, Artn D03201
959 Doi 10.1029/2006jd007436, 2007.
960
961 Peng, J., Hu, M., Guo, S., Du, Z., Zheng, J., Shang, D., Levy Zamora, M., Zeng, L., Shao, M., Wu,
962 Y.-S., Zheng, J., Wang, Y., Glen, C. R., Collins, D. R., Molina, M. J., and Zhang, R.: Markedly
963 enhanced absorption and direct radiative forcing of black carbon under polluted urban
964 environments, Proceedings of the National Academy of Sciences, 113, 4266-4271,
965 10.1073/pnas.1602310113, 2016.
966

967 Presto, A. A., Huff Hartz, K. E., and Donahue, N. M.: Secondary Organic Aerosol Production
968 from Terpene Ozonolysis. 2. Effect of NOx Concentration, Environ Sci Technol, 39, 7046-7054,
969 10.1021/es050400s, 2005.
970
971 Pye, Pinder, R. W., Piletic, I. R., Xie, Y., Capps, S. L., Lin, Y. H., Surratt, J. D., Zhang, Z. F.,
972 Gold, A., Luecken, D. J., Hutzell, W. T., Jaoui, M., Offenberg, J. H., Kleindienst, T. E.,
973 Lewandowski, M., and Edney, E. O.: Epoxide Pathways Improve Model Predictions of Isoprene
974 Markers and Reveal Key Role of Acidity in Aerosol Formation, Environ Sci Technol, 47, 11056-
975 11064, Doi 10.1021/Es402106h, 2013.
976
977 Pye, H. O. T., Chan, A. W. H., Barkley, M. P., and Seinfeld, J. H.: Global modeling of organic
978 aerosol: the importance of reactive nitrogen (NOx and NO3), Atmos Chem Phys, 10, 11261-11276,
979 DOI 10.5194/acp-10-11261-2010, 2010.
980
981 Pye, H. O. T., Luecken, D. J., Xu, L., Boyd, C. M., Ng, N. L., Baker, K. R., Ayres, B. R., Bash, J.
982 O., Baumann, K., Carter, W. P. L., Edgerton, E., Fry, J. L., Hutzell, W. T., Schwede, D. B., and
983 Shepson, P. B.: Modeling the Current and Future Roles of Particulate Organic Nitrates in the
984 Southeastern United States, Environ Sci Technol, 49, 14195-14203, 10.1021/acs.est.5b03738,
985 2015.
986
987 Robinson, N. H., Hamilton, J. F., Allan, J. D., Langford, B., Oram, D. E., Chen, Q., Docherty, K.,
988 Farmer, D. K., Jimenez, J. L., Ward, M. W., Hewitt, C. N., Barley, M. H., Jenkin, M. E., Rickard,
989 A. R., Martin, S. T., McFiggans, G., and Coe, H.: Evidence for a significant proportion of
990 Secondary Organic Aerosol from isoprene above a maritime tropical forest, Atmos Chem Phys,
991 11, 1039-1050, DOI 10.5194/acp-11-1039-2011, 2011a.
992
993 Robinson, N. H., Newton, H. M., Allan, J. D., Irwin, M., Hamilton, J. F., Flynn, M., Bower, K. N.,
994 Williams, P. I., Mills, G., Reeves, C. E., McFiggans, G., and Coe, H.: Source attribution of Bornean
995 air masses by back trajectory analysis during the OP3 project, Atmos. Chem. Phys., 11, 9605-9630,
996 10.5194/acp-11-9605-2011, 2011b.
997
998 Rollins, A. W., Browne, E. C., Min, K.-E., Pusede, S. E., Wooldridge, P. J., Gentner, D. R.,
999 Goldstein, A. H., Liu, S., Day, D. A., Russell, L. M., and Cohen, R. C.: Evidence for NOx Control
1000 over Nighttime SOA Formation, Science, 337, 1210-1212, 10.1126/science.1221520, 2012.
1001
1002 Saha, P. K., and Grieshop, A. P.: Exploring Divergent Volatility Properties from Yield and
1003 Thermodenuder Measurements of Secondary Organic Aerosol from α-Pinene Ozonolysis, Environ
1004 Sci Technol, 10.1021/acs.est.6b00303, 2016.
1005
1006 Sarrafzadeh, M., Wildt, J., Pullinen, I., Springer, M., Kleist, E., Tillmann, R., Schmitt, S. H., Wu,
1007 C., Mentel, T. F., Zhao, D., Hastie, D. R., and Kiendler-Scharr, A.: Impact of NOx and OH on
1008 secondary organic aerosol formation from β-pinene photooxidation, Atmos. Chem. Phys., 16,
1009 11237-11248, 10.5194/acp-16-11237-2016, 2016.

Sen, P. K.: Estimates of the Regression Coefficient Based on Kendall's Tau, Journal of the American Statistical Association, 63, 1379-1389, 10.1080/01621459.1968.10480934, 1968.

Slowik, J. G., Brook, J., Chang, R. Y. W., Evans, G. J., Hayden, K., Jeong, C. H., Li, S. M., Liggio, J., Liu, P. S. K., McGuire, M., Mihele, C., Sjostedt, S., Vlasenko, A., and Abbatt, J. P. D.: Photochemical processing of organic aerosol at nearby continental sites: contrast between urban plumes and regional aerosol, Atmos Chem Phys, 11, 2991-3006, DOI 10.5194/acp-11-2991-2011, 2011.

Spracklen, D. V., Jimenez, J. L., Carslaw, K. S., Worsnop, D. R., Evans, M. J., Mann, G. W., Zhang, Q., Canagaratna, M. R., Allan, J., Coe, H., McFiggans, G., Rap, A., and Forster, P.: Aerosol mass spectrometer constraint on the global secondary organic aerosol budget, Atmos. Chem. Phys., 11, 12109-12136, 10.5194/acp-11-12109-2011, 2011.

Surratt, J. D., Chan, A. W. H., Eddingsaas, N. C., Chan, M. N., Loza, C. L., Kwan, A. J., Hersey, S. P., Flagan, R. C., Wennberg, P. O., and Seinfeld, J. H.: Reactive intermediates revealed in secondary organic aerosol formation from isoprene, P Natl Acad Sci USA, 107, 6640-6645, DOI 10.1073/pnas.0911114107, 2010.

Tasoglou, A., and Pandis, S. N.: Formation and chemical aging of secondary organic aerosol during the β-caryophyllene oxidation, Atmos. Chem. Phys., 15, 6035-6046, 10.5194/acp-15-6035-2015, 2015.

Tsigaridis, K., Daskalakis, N., Kanakidou, M., Adams, P. J., Artaxo, P., Bahadur, R., Balkanski, Y., Bauer, S. E., Bellouin, N., Benedetti, A., Bergman, T., Berntsen, T. K., Beukes, J. P., Bian, H., Carslaw, K. S., Chin, M., Curci, G., Diehl, T., Easter, R. C., Ghan, S. J., Gong, S. L., Hodzic, A., Hoyle, C. R., Iversen, T., Jathar, S., Jimenez, J. L., Kaiser, J. W., Kirkevåg, A., Koch, D., Kokkola, H., Lee, Y. H., Lin, G., Liu, X., Luo, G., Ma, X., Mann, G. W., Mihalopoulos, N., Morcrette, J. J., Müller, J. F., Myhre, G., Myriokefalitakis, S., Ng, N. L., O'Donnell, D., Penner, J. E., Pozzoli, L., Pringle, K. J., Russell, L. M., Schulz, M., Sciare, J., Seland, Ø., Shindell, D. T., Sillman, S., Skeie, R. B., Spracklen, D., Stavrakou, T., Steenrod, S. D., Takemura, T., Tiitta, P., Tilmes, S., Tost, H., van Noije, T., van Zyl, P. G., von Salzen, K., Yu, F., Wang, Z., Wang, Z., Zaveri, R. A., Zhang, H., Zhang, K., Zhang, Q., and Zhang, X.: The AeroCom evaluation and intercomparison of organic aerosol in global models, Atmos. Chem. Phys., 14, 10845-10895, 10.5194/acp-14-10845-2014, 2014.

Tuet, W. Y., Chen, Y., Xu, L., Fok, S., Gao, D., Weber, R. J., and Ng, N. L.: Chemical oxidative potential of secondary organic aerosol (SOA) generated from the photooxidation of biogenic and anthropogenic volatile organic compounds, Atmos. Chem. Phys., 17, 839-853, 10.5194/acp-17-839-2017, 2017.

Ulbrich, I. M., Canagaratna, M. R., Zhang, Q., Worsnop, D. R., and Jimenez, J. L.: Interpretation of organic components from Positive Matrix Factorization of aerosol mass spectrometric data, Atmos. Chem. Phys., 9, 2891-2918, 10.5194/acp-9-2891-2009, 2009.

Vaden, T. D., Imre, D., Beránek, J., Shrivastava, M., and Zelenyuk, A.: Evaporation kinetics and phase of laboratory and ambient secondary organic aerosol, Proceedings of the National Academy of Sciences, 108, 2190-2195, 10.1073/pnas.1013391108, 2011.

Verma, V., Fang, T., Guo, H., King, L., Bates, J. T., Peltier, R. E., Edgerton, E., Russell, A. G., and Weber, R. J.: Reactive oxygen species associated with water-soluble PM2.5 in the southeastern United States: spatiotemporal trends and source apportionment, Atmos. Chem. Phys., 14, 12915-12930, 10.5194/acp-14-12915-2014, 2014.

Visser, S., Slowik, J. G., Furger, M., Zotter, P., Bukowiecki, N., Canonaco, F., Flechsig, U., Appel, K., Green, D. C., Tremper, A. H., Young, D. E., Williams, P. I., Allan, J. D., Coe, H., Williams, L. R., Mohr, C., Xu, L., Ng, N. L., Nemitz, E., Barlow, J. F., Halios, C. H., Fleming, Z. L., Baltensperger, U., and Prévôt, A. S. H.: Advanced source apportionment of size-resolved trace elements at multiple sites in London during winter, Atmos. Chem. Phys., 15, 11291-11309, 10.5194/acp-15-11291-2015, 2015.

Warneke, C., Trainer, M., de Gouw, J. A., Parrish, D. D., Fahey, D. W., Ravishankara, A. R., Middlebrook, A. M., Brock, C. A., Roberts, J. M., Brown, S. S., Neuman, J. A., Lerner, B. M., Lack, D., Law, D., Hübler, G., Pollack, I., Sjostedt, S., Ryerson, T. B., Gilman, J. B., Liao, J., Holloway, J., Peischl, J., Nowak, J. B., Aikin, K. C., Min, K. E., Washenfelder, R. A., Graus, M. G., Richardson, M., Markovic, M. Z., Wagner, N. L., Welti, A., Veres, P. R., Edwards, P., Schwarz, J. P., Gordon, T., Dube, W. P., McKeen, S. A., Brioude, J., Ahmadov, R., Bougiatioti, A., Lin, J. J., Nenes, A., Wolfe, G. M., Hanisco, T. F., Lee, B. H., Lopez-Hilfiker, F. D., Thornton, J. A., Keutsch, F. N., Kaiser, J., Mao, J., and Hatch, C. D.: Instrumentation and measurement strategy for the NOAA SENEX aircraft campaign as part of the Southeast Atmosphere Study 2013, Atmos. Meas. Tech., 9, 3063-3093, 10.5194/amt-9-3063-2016, 2016.

Weber, R. J., Sullivan, A. P., Peltier, R. E., Russell, A., Yan, B., Zheng, M., de Gouw, J., Warneke, C., Brock, C., Holloway, J. S., Atlas, E. L., and Edgerton, E.: A study of secondary organic aerosol formation in the anthropogenic-influenced southeastern United States, J Geophys Res-Atmos, 112, Artn D13302 Doi 10.1029/2007jd008408, 2007.

Xu, L., Guo, H., Boyd, C. M., Klein, M., Bougiatioti, A., Cerully, K. M., Hite, J. R., Isaacman-VanWertz, G., Kreisberg, N. M., Knote, C., Olson, K., Koss, A., Goldstein, A. H., Hering, S. V., de Gouw, J., Baumann, K., Lee, S.-H., Nenes, A., Weber, R. J., and Ng, N. L.: Effects of anthropogenic emissions on aerosol formation from isoprene and monoterpenes in the southeastern United States, Proceedings of the National Academy of Sciences, 112, 37-42, 10.1073/pnas.1417609112, 2015a.

Xu, L., Suresh, S., Guo, H., Weber, R. J., and Ng, N. L.: Aerosol characterization over the southeastern United States using high-resolution aerosol mass spectrometry: spatial and seasonal variation of aerosol composition and sources with a focus on organic nitrates, Atmos. Chem. Phys., 15, 7307-7336, 10.5194/acp-15-7307-2015, 2015b.

Xu, L., Middlebrook, A. M., Liao, J., de Gouw, J. A., Guo, H., Weber, R. J., Nenes, A., Lopez-Hilfiker, F. D., Lee, B. H., Thornton, J. A., Brock, C. A., Neuman, J. A., Nowak, J. B., Pollack, I. B., Welti, A., Graus, M., Warneke, C., and Ng, N. L.: Enhanced formation of isoprene-derived organic aerosol in sulfur-rich power plant plumes during Southeast Nexus, Journal of Geophysical Research: Atmospheres, 121, 11,137-111,153, 10.1002/2016JD025156, 2016a.

Xu, L., Williams, L. R., Young, D. E., Allan, J. D., Coe, H., Massoli, P., Fortner, E., Chhabra, P., Herndon, S., Brooks, W. A., Jayne, J. T., Worsnop, D. R., Aiken, A. C., Liu, S., Gorkowski, K., Dubey, M. K., Fleming, Z. L., Visser, S., Prévôt, A. S. H., and Ng, N. L.: Wintertime aerosol chemical composition, volatility, and spatial variability in the greater London area, Atmos. Chem. Phys., 16, 1139-1160, 10.5194/acp-16-1139-2016, 2016b.

Xu, W., Han, T., Du, W., Wang, Q., Chen, C., Zhao, J., Zhang, Y., Li, J., Fu, P., Wang, Z., Worsnop, D. R., and Sun, Y.: Effects of Aqueous-Phase and Photochemical Processing on Secondary Organic Aerosol Formation and Evolution in Beijing, China, Environ Sci Technol, 10.1021/acs.est.6b04498, 2016c.

Yu, J., Cocker, D. R., Griffin, R. J., Flagan, R. C., and Seinfeld, J. H.: Gas-Phase Ozone Oxidation of Monoterpenes: Gaseous and Particulate Products, J Atmos Chem, 34, 207-258, 10.1023/a:1006254930583, 1999.

Zhang, H., Yee, L. D., Lee, B. H., Curtis, M. P., Worton, D. R., Isaacman-VanWertz, G., Offenberg, J. H., Lewandowski, M., Kleindienst, T. E., Beaver, M. R., Holder, A. L., Lonneman, W. A., Docherty, K. S., Jaoui, M., Pye, H. O. T., Hu, W., Day, D. A., Campuzano-Jost, P., Jimenez, J. L., Guo, H., Weber, R. J., de Gouw, J., Koss, A. R., Edgerton, E. S., Brune, W., Mohr, C., Lopez-Hilfiker, F. D., Lutz, A., Kreisberg, N. M., Spielman, S. R., Hering, S. V., Wilson, K. R., Thornton, J. A., and Goldstein, A. H.: Monoterpenes are the largest source of summertime organic aerosol in the southeastern United States, Proceedings of the National Academy of Sciences, 10.1073/pnas.1717513115, 2018.

Zhang, Q., Jimenez, J. L., Canagaratna, M. R., Allan, J. D., Coe, H., Ulbrich, I., Alfarra, M. R., Takami, A., Middlebrook, A. M., Sun, Y. L., Dzepina, K., Dunlea, E., Docherty, K., DeCarlo, P. F., Salcedo, D., Onasch, T., Jayne, J. T., Miyoshi, T., Shimono, A., Hatakeyama, S., Takegawa, N., Kondo, Y., Schneider, J., Drewnick, F., Borrmann, S., Weimer, S., Demerjian, K., Williams, P., Bower, K., Bahreini, R., Cottrell, L., Griffin, R. J., Rautiainen, J., Sun, J. Y., Zhang, Y. M., and Worsnop, D. R.: Ubiquity and dominance of oxygenated species in organic aerosols in anthropogenically-influenced Northern Hemisphere midlatitudes, Geophysical Research Letters, 34, Artn L13801 Doi 10.1029/2007gl029979, 2007.

Zhang, X., Cappa, C. D., Jathar, S. H., McVay, R. C., Ensberg, J. J., Kleeman, M. J., and Seinfeld, J. H.: Influence of vapor wall loss in laboratory chambers on yields of secondary organic aerosol, Proceedings of the National Academy of Sciences, 10.1073/pnas.1404727111, 2014.

Zhang, X., McVay, R. C., Huang, D. D., Dalleska, N. F., Aumont, B., Flagan, R. C., and Seinfeld, J. H.: Formation and evolution of molecular products in α-pinene secondary organic aerosol, Proceedings of the National Academy of Sciences, 112, 14168-14173, 10.1073/pnas.1517742112, 2015.

Zheng, Y., Unger, N., Hodzic, A., Emmons, L., Knote, C., Tilmes, S., Lamarque, J. F., and Yu, P.: Limited effect of anthropogenic nitrogen oxides on secondary organic aerosol formation, Atmos. Chem. Phys., 15, 13487-13506, 10.5194/acp-15-13487-2015, 2015.

Zotter, P., El-Haddad, I., Zhang, Y., Hayes, P. L., Zhang, X., Lin, Y.-H., Wacker, L., Schnelle-Kreis, J., Abbaszade, G., Zimmermann, R., Surratt, J. D., Weber, R., Jimenez, J. L., Szidat, S., Baltensperger, U., and Prévôt, A. S. H.: Diurnal cycle of fossil and nonfossil carbon using radiocarbon analyses during CalNex, Journal of Geophysical Research: Atmospheres, 119, 2013JD021114, 10.1002/2013JD021114, 2014.

## Appendix A. Data Analysis Method for Perturbation Experiments

The most challenging and important analysis is to determine if the perturbation results in a statistically significant change in the mass concentration of OA factors. We perform the following analysis to calculate the changes in the mass concentration of OA factors after perturbation, to determine if the change is significant, and to evaluate if the change is simply due to ambient variation.

The duration of one perturbation experiment is about 130min, including four periods: Amb_Bf (~30min), Chamber_Bf (~30min), Chamber_Af (~40min), and Amb_Af (~30min), as illustrated in Fig. A1. Firstly, we assume that the ambient variation is linear during both the Chamber_Bf and Chamber_Af periods (i.e., when instruments are connected to chamber and not sampling the ambient aerosol) and that the ambient variation can be represented by interpolating Amb_Bf and Amb_Af. The validity of this assumption will be discussed shortly. To obtain the slope of ambient variation, we analyze the combined Amb_Bf and Amb_Af data and use Theil-Sen estimator(Sen, 1968). The Theil-Sen estimator is a method to robustly fit a line to a set of two-dimensional points (i.e., concentration "$C$" and time "$t$" in this study). This method chooses the median of the slopes $(C_j-C_i)/(t_j-t_i)$ determined by all pairs of sample points. Compared to simple linear regression using ordinary least squares, the Theil-Sen estimator is robust and insensitive to outliers. Unless specifically noted, the slope is Appendix A is calculated from Theil-Sen estimator. Secondly, we use the slope to extrapolate the Chamber_Bf data to estimate aerosol concentration inside the chamber during the Chamber_Af period if there were no VOC injection. We refer to this estimated aerosol concentration as "extrapolated Chamber_Bf" and use it as the reference to calculate the change in aerosol mass concentration after perturbation. We extrapolate the Chamber_Bf data, instead of ambient data, because the OA concentration in chamber is lower than that in the atmosphere due to wall loss. Thirdly, we calculate the changes in the concentration of OA factors based on the difference between measured Chamber_Af data and "extrapolated Chamber_Bf".

For each perturbation experiment, after calculating the changes in the concentration of OA factors, we develop a set of criteria to determine if the changes are statistically significant and if the changes are simply due to ambient variation. The increase in the concentration of an OA factor

needs to satisfy all criteria to be considered as statistically significant and not due to ambient variation.

**Criterion 1**: The difference in concentration between Chamber_Af and extrapolated Chamber_Bf must be significant. We use T-test and 95% confidence interval.

**Criterion 2**: The slope of all data points or the first 8 data points during the Chamber_Af period is significantly different from the slope of aerosol concentration during the Chamber_Bf period. The rationale behind this criterion is that if the perturbation causes a substantial change in the concentration of an OA factor, its slope during the Chamber_Af period should be different from that during the Chamber_Bf period.

The slope of aerosol concentration during the Chamber_Af period is obtained in the following way. We calculate the slope by using (1) all data points and (2) only first 8 data points during the Chamber_Af period. This is because the concentration of factors firstly increases after perturbation and then decreases due to dilution (Fig. A1). In this case, the slope obtained by fitting all data points might be negative and will not reflect the initial increase in concentration (e.g., LO-OOA of ap_0805_1 in Fig. S9a). Using only the first few data points during the Chamber_Af period can avoid this issue. We select the first 8 data points in this period because the concentrations of total OA and OA factors typically reach the highest at the 8th point (i.e., ~16min after injection). The slope is calculated by Theil-Sen estimator.

The slope of aerosol concentration during the Chamber_Bf period is analyzed in the following way. In order to determine if the slope in Chamber_Af is significantly different from that in Chamber_Bf, we use bootstrap analysis (1000 times) to obtain a distribution of the slope of Chamber_Bf. In brief, in each random resampling of Chamber_Bf with replacement, a slope is calculated by Theil-Sen estimator. Then, 1000 times resampling provides a distribution of slope in Chamber_Bf. The 5% and 95% percentiles of the slope distribution are compared to the slope of Chamber_Af to determine if the slopes are significantly different. If the slope of Chamber_Af (from either all data points or the first 8 data points) is smaller (or larger) than the 5% (or 95%) percentile, the slopes in Chamber_Bf and Chamber_Af are significantly different.

**Criterion 3**: The slope of all data points or the first 8 data points during the Chamber_Af period is significantly different from the slope of ambient data (i.e., combined Amb_Bf and Amb_Af). The rationale behind this criterion is the same as the second criterion. That is, if the perturbation

causes a substantial change in the concentration of an OA factor, its slope during the Chamber_Af period should be different from that in ambient data. The procedure to obtain a distribution of slopes in the ambient data (combined Amb_Bf and Amb_Af) is same as Criterion 2.

As mentioned above, one critical assumption is that the ambient variation is linear during both the Chamber_Bf and Chamber_Af periods (i.e., when instruments are connected to chamber and not sampling the ambient aerosol) and that the ambient variation can be represented by interpolating Amb_Bf and Amb_Af. We design the following pseudo-experiment to test the validity of this assumption. In brief, we perform the same analysis as we did for the perturbation experiments, but using ambient data **only** (i.e., no perturbation data). We firstly randomly select a data point, which defines the start point of one pseudo-test. Secondly, based on the start point, we obtain the concentration of OA factors during "Amb_Bf" period, (i.e., from start point to start point + 30min), "Chamber_Bf" period (i.e., from start point + 30min to start point + 60min), "Chamber_Af" period (i.e., from start point + 60min to start point + 100min), and "Amb_Af" period (from start point + 100 min to start point + 130min). This mimics the sampling periods in a real perturbation experiment. Thirdly, we calculate the slope of ambient period (i.e., combined "Amb_Bf" and "Amb_Af" periods) and the slope of chamber period (i.e., combined "Chamber_Bf" and "Chamber_Af" periods) in the pseudo-test. Fourthly, we calculate if the slope of chamber period is significantly different from the slope of ambient period. We repeat this pseudo-test 1000 times and then obtain the probability of whether the slopes of chamber period and ambient period are significantly different.

Fig. A2a shows the probability that the slopes of chamber period and ambient period are not significantly different for five factors. The larger this probability is, the more reliable the linearity assumption is. The average probability is ~50% for all factors, without discernible diurnal trends. This suggest that there is ~50% chance that the linear variation assumption is valid. Since the linearity assumption is not perfect, we develop another criterion to constrain the potential influence of ambient variation on the interpretation of perturbation results.

**Criterion 4**: From the above pseudo-experiment on ambient data only, we can calculate the relative change in slope between "chamber period" and "ambient period" by

$$\text{relative change in slope} = \frac{\text{Slope}_{\text{Chamber}} - \text{Slope}_{\text{Amb}}}{\text{Slope}_{\text{Amb}}} \quad \text{Eqn 1}$$

In each pseudo-experiment test, we calculate a relative change in slope between "chamber period" and "ambient period". By repeating the pseudo-experiment test 1000 times, we obtain a frequency distribution of the relative change in slope for each OA factor (Fig. A2b). This frequency distribution indicates the probability that certain relative change in slope occurs due to ambient variation. Take LO-OOA as an example, the probability that the relative change in slope varies by a factor 8 due to ambient variation is ~1%. Thus, if the relative change in slope of LO-OOA in a α-pinene experiment is 8, the change is unlikely due to ambient variation. We use the 5% and 95% percentiles from the frequency distribution as the fourth criterion to determine if the changes in the concentrations of OA factors in each perturbation experiment are due to ambient variation. In other words, if the relative change in slope between Chamber_Af and ambient data in a real perturbation experiment falls outside of the 5% or 95% percentiles, the changes in the concentrations of OA factors are likely due to perturbing chamber with VOC, instead of ambient variation. This criterion strictly considers the influence of ambient variation. In general, the comparison in slope is an optimal option to account for ambient variation, because the influence of ambient variation is unlikely to coincide with the perturbation.

Based on these 4 criteria, the OA factors with significant changes in their mass concentrations as a result of perturbation are shown in Fig. 4. LO-OOA is enhanced in 14 out of 19 α-pinene experiments. However, total OA is only enhanced in 8 out of 19 α-pinene experiments. Several reasons can contribute to the different behaviors of LO-OOA and OA. Firstly, as total OA has multiple sources, the enhancement in one factor does not guarantee an enhancement of total OA. For instance, in some perturbation experiments, while LO-OOA is enhanced, the concentration of other factors steadily decreases due to ambient variation. The increase in LO-OOA and decrease in other factors compensate each other and result in a lack of enhancement in total OA. Secondly, based on the pseudo-experiment, we note that total OA is more easily affected by ambient variation than a single OA factor. For example, the 95% of the relative change in slope of total OA is 3.59, which is larger than any OA factors (Fig. A2b). Thus, the criteria for the change in total OA concentration to be considered as significant are stricter than those for a single OA factor. Thus, some experiments with significant changes in LO-OOA do not have significant changes in total OA.

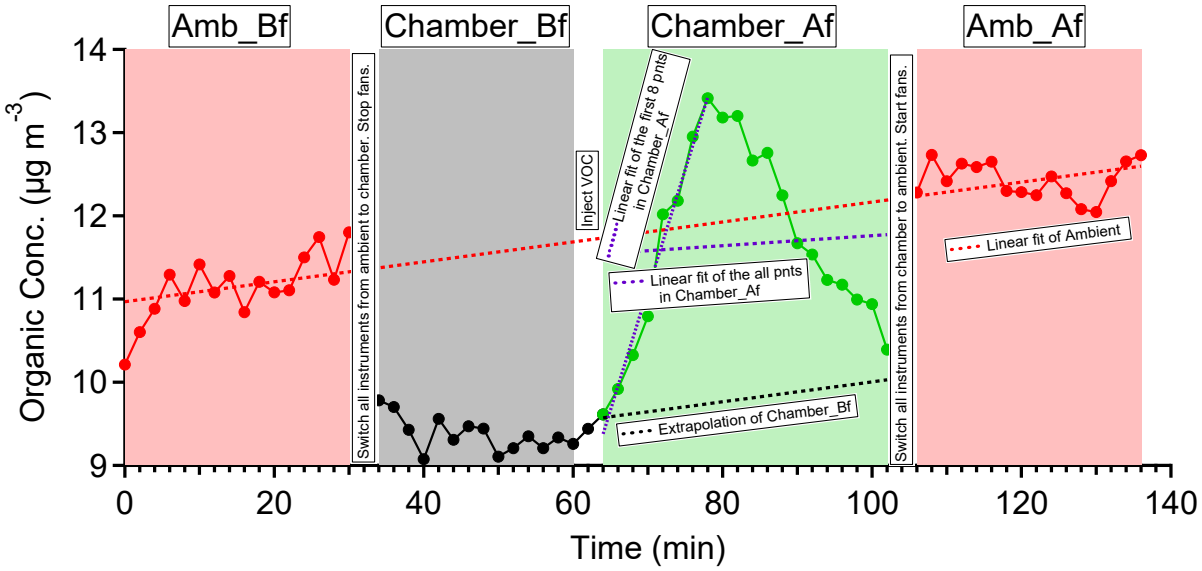


Fig. A1. Time series of OA in experiment ap_0801_1 to illustrate the analysis method. Each perturbation experiment includes four periods: Amb_Bf (~30min), Chamber_Bf (~30min), Chamber_Af (~40min), and Amb_Af (~40min). "Amb" and "Chamber" correspond to the periods when the instruments are sampling ambient and chamber, respectively. "Bf" and "Af" stand for before and after perturbation, respectively. The solid lines are measurement data. The dashed red lines are the linear fit of ambient data (i.e., combined Amb_Bf and Amb_Af). The slope is used to extrapolate Chamber_Bf data to Chamber_Af period (i.e., black dashed line). The dense dashed purple line is the linear fit of the first 8 points during the Chamber_Af period. The sparse dashed purple line is the linear fit of all data points during the Chamber_Af period. During this period, the difference between measurements (i.e., solid green data points) and extrapolated Chamber_Bf (i.e., dashed black line) represents the change in organic concentration caused by perturbation.

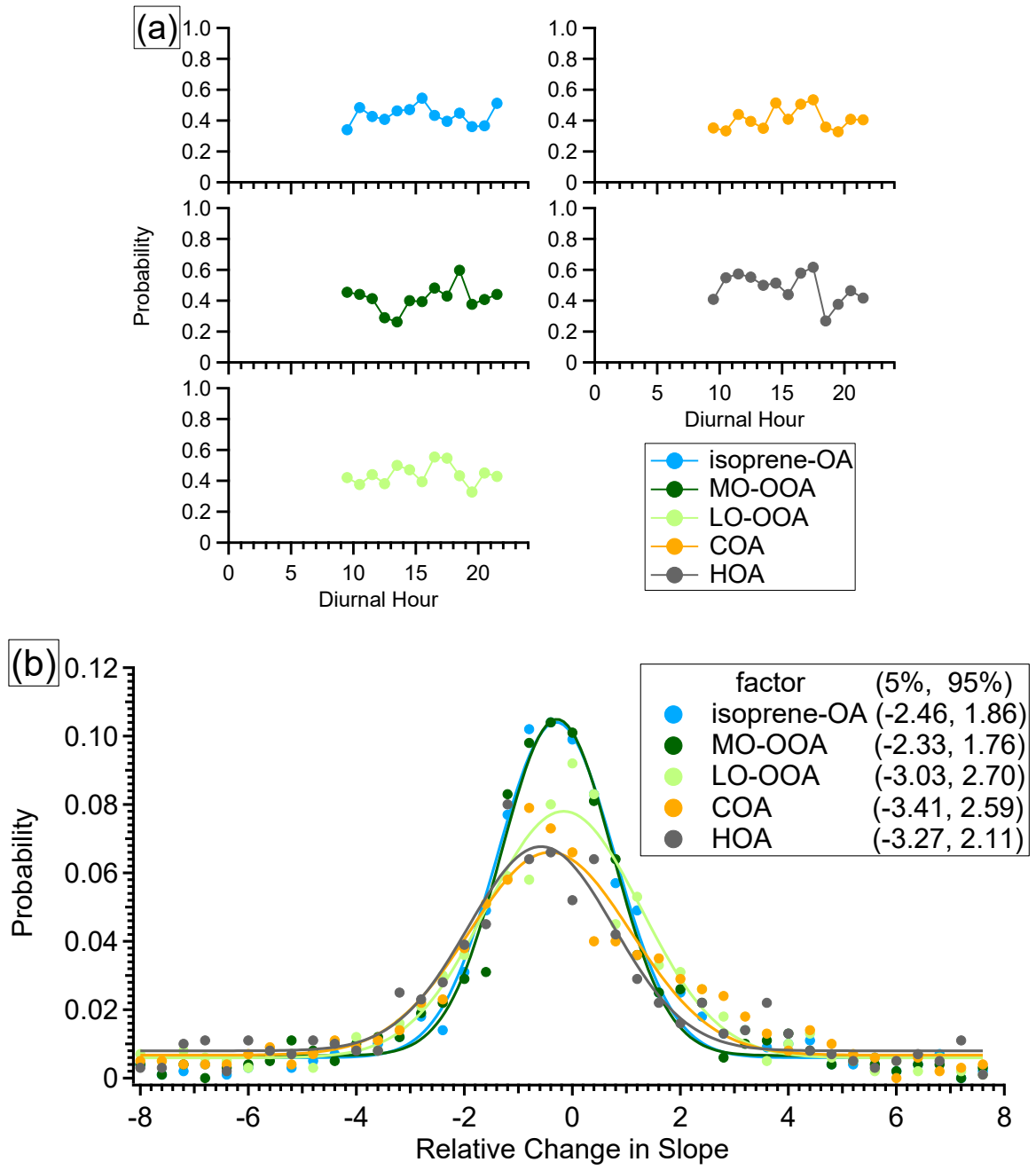


Fig. A2. (a) The diurnal trends of the probability that the slopes between ambient periods (i.e., Amb_Bf and Amb_Af periods) and chamber periods (i.e., Chamber_Bf and Chamber_Af periods) are not significantly different in the pseudo-experiment. (b) The frequency distribution of the relative change in slope. The data points are fitted using Gaussian function. The numbers in the box represent the 5% and 95% percentile of the Gaussian fit.

## Appendix B. Ambient Perturbation Experiments with Acidic Sulfate Particles

Previous field observations showed strong correlation between isoprene-OA and sulfate (Xu et al., 2015a; Xu et al., 2016a; Budisulistiorini et al., 2015). Moreover, airborne measurements over power plant plumes in Georgia, U.S. observed enhanced isoprene-OA formation in the sulfate-rich power plant plume (Xu et al., 2016a). To probe the relationship between isoprene-OA and sulfate, we conducted perturbation experiments in August 2015 by injecting acidic sulfate particles (i.e., a mixture of $H_2SO_4$ and $MgSO_4$) into the 2 $m^3$ Teflon chamber. This mimics the airborne measurements over power plants, which introduce sulfate into the atmosphere (Xu et al., 2016a).

The experimental procedure in 2015 experiments is generally similar to those in 2016 experiments, but has the following modifications. Firstly, in order to avoid the depletion of species which can uptake to sulfate particles, we kept one fan on during the Chamber_Bf and Chamber_Af periods to enhance the air exchange between chamber and atmosphere. Secondly, considering the fan is on during sulfate injection to enhance mixing chamber air with ambient air, we only use the Chamber_Bf and Chamber_Af periods to calculate the changes in OA factors. The Criteria (1)(2)(4) are applied in 2015 experiments. Thirdly, the Chamber_Bf period is ~40 min in 2015 experiments, which is slightly longer than the 30 min in 2016 experiments. Fourthly, the HR-ToF-CIMS was not deployed in 2015 experiments.

The acidic sulfate seed particles were introduced into chamber by atomizing 0.88mM $H_2SO_4$ + 0.48mM $MgSO_4$ mixture solution from a nebulizer (U-5000AT, Cetac Technologies Inc., Omaha, Nebraska, USA). One important interference in these sulfate perturbation experiments is the trace amount of organics in solvent water [i.e., HPLC-grade ultrapure water (Baker Inc.)], which is used to prepare the $H_2SO_4$+$MgSO_4$ solution. These organics were injected into chamber together with sulfate. We utilize the multilinear engine solver (ME-2) to constrain the organics from solvent water (i.e., $H_2O$-Org). Unlike the PMF2 solver which does not require any a priori information of mass spectrum or time series, the ME-2 solver uses a priori information to reduce rotational ambiguity among possible solutions(Canonaco et al., 2013; Paatero, 1999). We obtained the reference spectrum of organic contamination (i.e., the a priori information for ME-2 solver) by atomizing the $H_2SO_4$+$MgSO_4$ solution directly into AMS. The ME-2 solver successfully extracted a factor (i.e., denoted as $H_2O$-Org factor, Fig. B1), which showed a clear enhanced concentration during atomization (Fig. B2).

A total of four experiments were performed and details are summarized in Table B1. As shown in Fig. B2, the isoprene-OA factor increases in all three daytime experiments, but not the nighttime experiment. Based on current understanding of isoprene-OA factor, this enhancement is likely due to the reactive uptake of IEPOX. The lack of enhancement in nighttime experiment is consistent with low IEPOX concentration at night (Hu et al., 2015). Our results provide direct observational evidence that acidic sulfate particles lead to increase in isoprene-OA, which supports results from previous studies (Xu et al., 2015a; Xu et al., 2016a; Budisulistiorini et al., 2015). Due to lack of measurements of gas-phase organic compounds, we are unable to identify the reactive species. Other species, such as glyoxal (Kroll et al., 2005), isoprene hydroperoxides (Liu et al., 2016), and HOMs (Ehn et al., 2014), also have the potential to uptake to acidic sulfate particles and form SOA. Future experiments with comprehensive measurements of gas-phase organic compounds can provide more insights into the identities of reactive uptake species.

We note that in non-atomizing period, the concentration of $H_2O$-Org factor is close to zero, but not zero. Since $H_2O$-Org arises from the atomizing solution, it should only exist during atomizing periods. Thus, the non-zero concentration suggests the limitation of the ME-2 solver and cautions are required when using ME-2 solver to resolve one factor based on a specific mass spectrum. This limitation does not affect the conclusion that the enhancement in isoprene-OA is likely due to the reactive uptake of organic species, as we further verify that the organic increase in three daytime perturbation experiments with sulfate particles cannot be solely explained by the organic contamination in atomizing water, from the following two aspects. For example, we atomize the solution directly into AMS and find that the Org/$SO_4$ ratio is 0.025. This value is significantly lower than the Org/$SO_4$ ratio in the three daytime sulfate perturbation experiments (i.e., 0.048-0.059), but close to the nighttime sulfate perturbation experiment (i.e., 0.022) (Fig. B4).

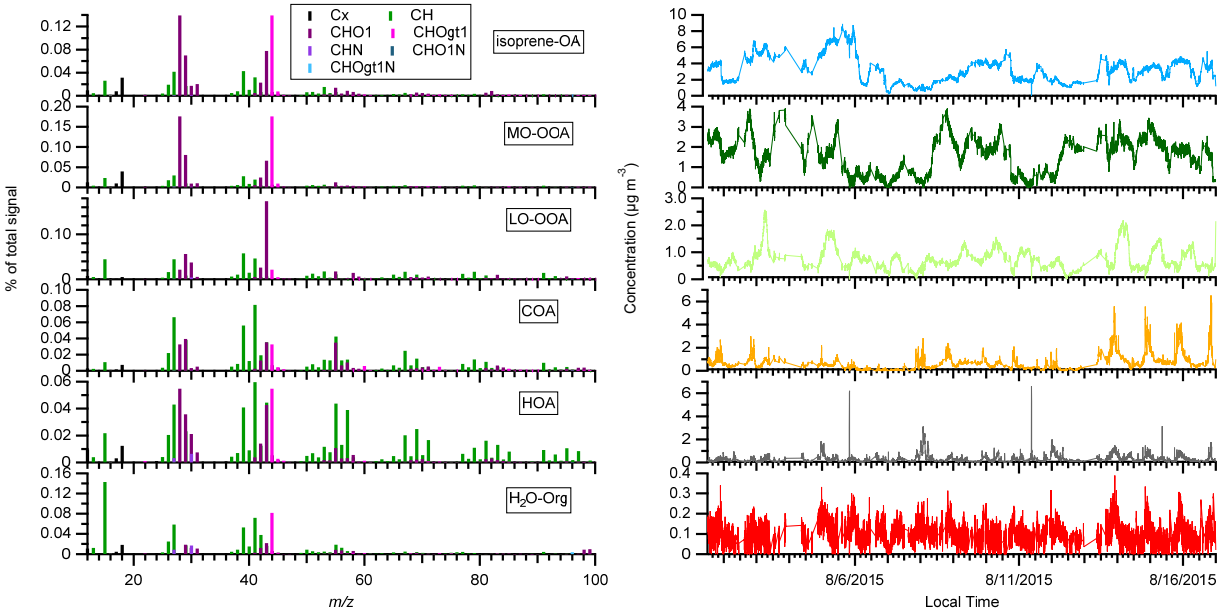


1357

1358 Fig. B1. The mass spectra and time series of OA factors in the 2015 acidic sulfate particle
1359 perturbation measurements. Note that the perturbation periods are included in the time series.

1360

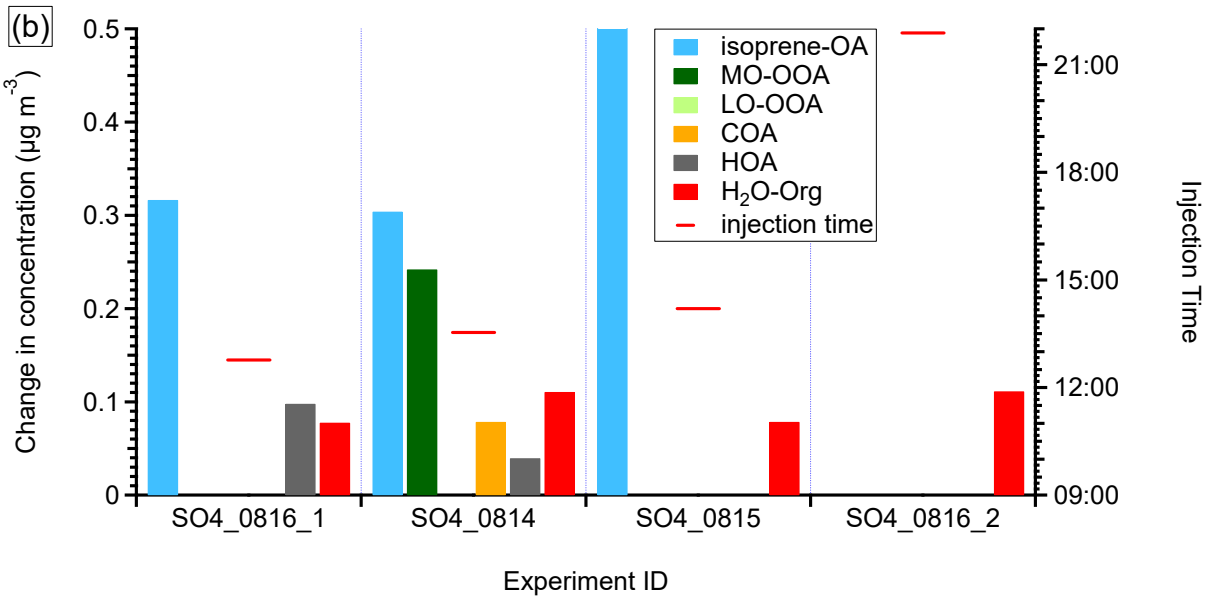


Fig. B2. The statistically significant changes in the concentrations of OA factors after perturbation by acidic sulfate particles. The experiments are sorted by perturbation time. The changes in concentration are the difference between measurements during the Chamber_Af period and mass concentration extrapolated from the Chamber_Bf period. A set of criteria are developed to evaluate if the changes are significant and if the changes are due to ambient variation (Appendix A). $H_2O$-Org factor in these sulfate perturbation experiments represents organic contaminations in atomizing water.

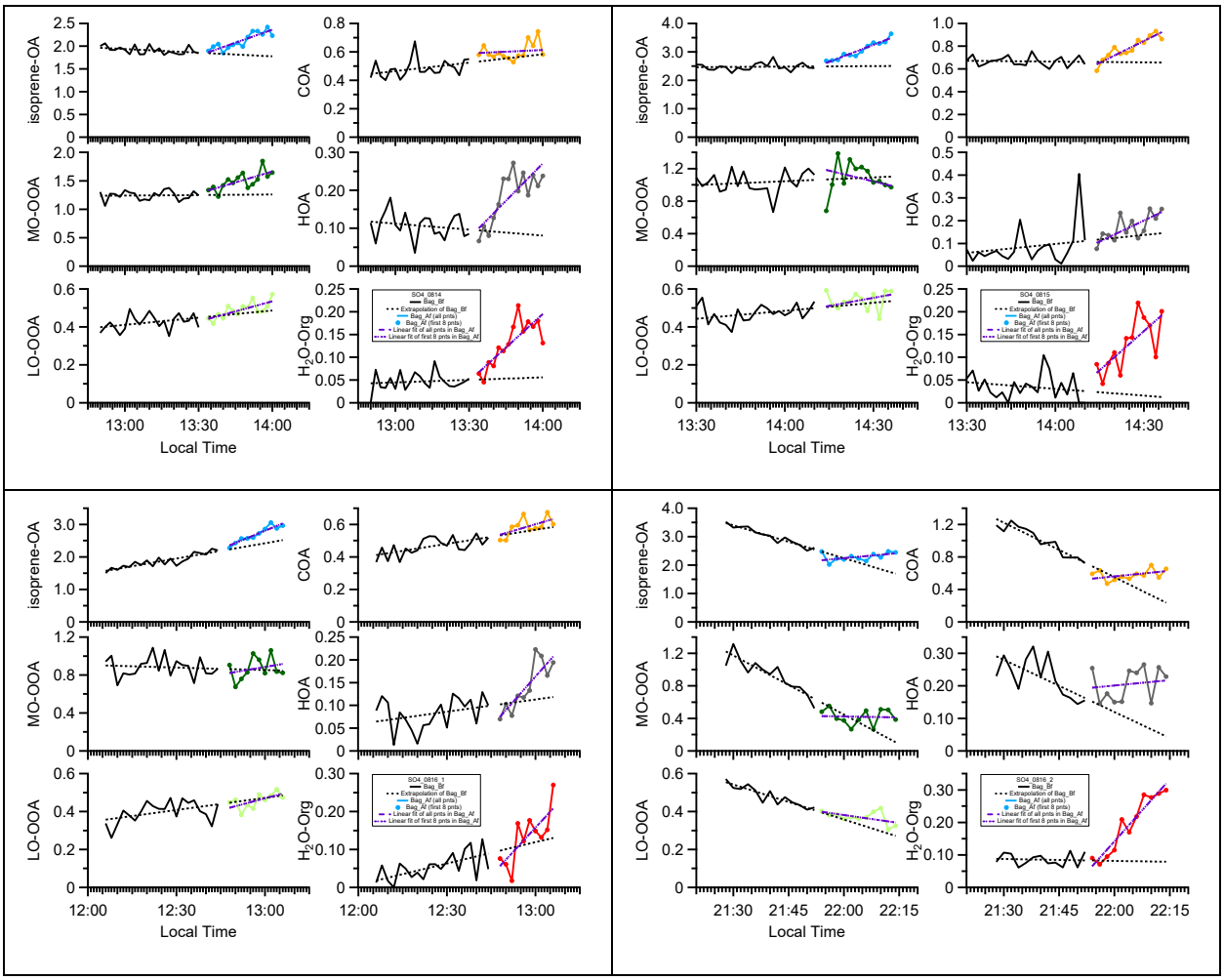


Fig. B3. Time series of OA factors in each sulfate perturbation experiment.

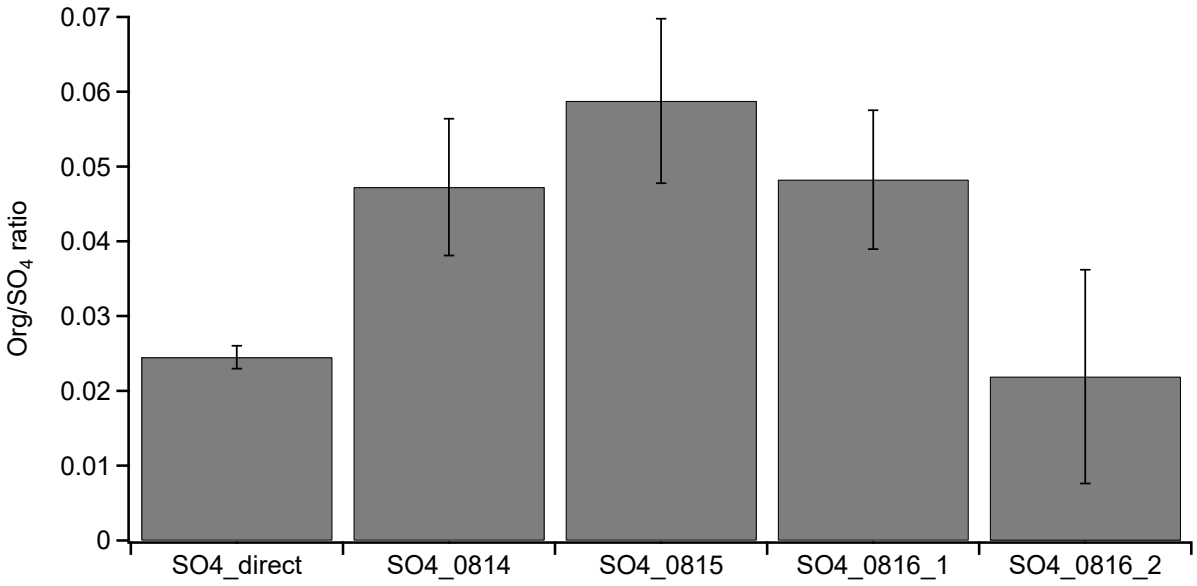


Fig. B4. The Org/$SO_4$ ratio in sulfate perturbation experiments and laboratory tests by directly atomizing $H_2SO_4$ + $MgSO_4$ mixture solution into AMS (i.e., SO4_direct).

Table B1. Experimental conditions for sulfate perturbation experiments.

| Perturbation | Expt ID[a] | Date | Injection Time | Perturbation Amount[b] | NO[c] (ppb) | $NO_2$[c] (ppb) | $O_3$[c] (ppb) |
|---|---|---|---|---|---|---|---|
| sulfate | SO4_0814 | 8/14/2015 | 13:32 | 16.29 | 0.51 | 5.86 | 59.8 |
| | SO4_0815 | 8/15/2015 | 14:12 | 14.33 | 0.18 | 4.79 | 63.0 |
| | SO4_0816_1 | 8/16/2015 | 12:46 | 14.52 | 0.36 | 4.08 | 53.2 |
| | SO4_0816_2 | 8/16/2015 | 21:53 | 13.92 | 0.03 | 5.40 | 35.6 |

[a]Expt ID is named as "perturbation species + date + experiment number". For example, SO4_0816_1 represents the first sulfate perturbation experiment on 08/16.

[b]The unit for the perturbation in sulfate experiments is $\mu g\ m^{-3}$. The perturbation amounts of sulfate are calculated from Chamber_Af – extrapolated Chamber_bf.

[c]Average concentration during the Chamber_Af period.